

1           **Continuous separation of land use and climate effects on the water balance using**  
2   **principal components regression**

3 Samuel C. Zipper<sup>1,2,3,\*</sup>, Melissa Motew<sup>4</sup>, Eric G. Booth<sup>1,5</sup>, Xi Chen<sup>4,6</sup>, Jiangxiao Qiu<sup>7</sup>, Christopher J.  
4 Kucharik<sup>4,5</sup>, Stephen R. Carpenter<sup>9</sup>, Steven P. Loheide II<sup>1</sup>

5 \* Corresponding author: samuelczipper@gmail.com

6 <sup>1</sup> Department of Civil & Environmental Engineering, University of Wisconsin-Madison, Madison WI,  
7 USA.

8 <sup>2</sup> Department of Civil Engineering, University of Victoria, Victoria BC, Canada

9 <sup>3</sup> Department of Earth & Planetary Sciences, McGill University, Montreal QC, Canada

10 <sup>4</sup> Nelson Institute Center for Sustainability and the Global Environment, University of Wisconsin-  
11 Madison, Madison WI, USA

12 <sup>5</sup> Department of Agronomy, University of Wisconsin-Madison, Madison WI, USA

13 <sup>6</sup> Department of Geography, University of Cincinnati, Cincinnati OH, USA

14 <sup>7</sup> School of Forest Resources & Conservation, Fort Lauderdale Research and Education Center,  
15 University of Florida, Fort Lauderdale FL, USA

16 <sup>8</sup> Department of Zoology, University of Wisconsin-Madison, Madison WI, USA

17 <sup>9</sup> Center for Limnology, University of Wisconsin-Madison, Madison WI, USA

18 **Keywords:** land use change; climate change; streamflow; evapotranspiration; baseflow; urbanization;  
19

## 20 Abstract

21 Understanding the combined and separate effects of climate and land use change on the water cycle is  
22 necessary to mitigate negative impacts. However, existing methodologies typically divide data into  
23 discrete (before and after) periods, implicitly representing climate and land use as step changes when in  
24 reality these changes are often gradual. Here, we introduce a new principal components regression-based  
25 methodology designed to separate climate and land use effects on any hydrological flux of interest  
26 continuously through time. We present two applications in the Yahara River watershed (Wisconsin, USA)  
27 to better understand synergistic or antagonistic relationships between land use and climate: (1) historical  
28 streamflow in an urbanizing subwatershed; and (2) simulated future evapotranspiration, drainage, and  
29 direct runoff from a suite of contrasting climate and land use scenarios for the entire watershed. In the  
30 historical analysis for the subwatershed, we show that 60% of recent streamflow changes can be attributed  
31 to climate, but baseflow is significantly increasing through time due to land use change and long-term  
32 increases in groundwater storage. For the watershed, simulation results indicate all components of the  
33 future water balance will respond more strongly to changes in climate than land use, with the largest  
34 potential land use effects on drainage. These results indicate that diverse land use change trajectories may  
35 counteract each other while the effects of climate are more homogeneous at watershed scales. Therefore,  
36 management opportunities to counteract climate change effects will likely be more effective at smaller  
37 spatial scales, where land use trajectories are monodirectional.

## 38 1. Introduction

39 Climate and land use (which we define broadly to include land use, land cover, and land management) are  
40 two major drivers of global hydrological change (Foley, 2005; Steffen et al., 2015; Vörösmarty et al.,  
41 2000). While economic, governmental, and social pressures may be exogenous to a watershed, land use  
42 can be controlled by decision-making at local levels (individual, city, county, and state). In contrast,  
43 climate change is driven by global emissions, which requires a coordinated effort well beyond an  
44 individual watershed to address. Therefore, land use decisions may be a viable path to mitigating  
45 undesirable impacts of climate change on the water cycle at watershed scales.

46 While several point-based studies have found significant impacts of land use change on the water balance  
47 (Giménez et al., 2016; Noretto et al., 2012; Scanlon et al., 2005; Twine et al., 2004), most watershed-  
48 scale studies which attempt to disentangle the impacts of climate and land use have found that the impact  
49 of climate change on hydrology outweighs that of land use change, particularly where there are strong  
50 changes in precipitation (Chawla & Mujumdar, 2015; Jiang et al., 2015; Li et al., 2009; Mango et al.,  
51 2011; Tao et al., 2014; Wu et al., 2015; Yang et al., 2017). Thus, there is a growing acknowledgment that  
52 the impacts of land use change are superimposed on a larger climate trend, and can either amplify or  
53 partially counteract the impacts of climate change (Gyawali et al., 2015; Juckem et al., 2008; Martin et  
54 al., 2017; Shi et al., 2012; Tomer & Schilling, 2009; Zhang et al., 2016). In particular, land use may be  
55 most important locally (Frans et al., 2013; Haddeland et al., 2007; Peterson et al., 2011; Xu et al., 2013),  
56 during wet/dry extremes (Villarini & Strong, 2014), or where significant infrastructure projects (e.g.  
57 dams) occur (Wu et al., 2012; Ye et al., 2003).

58 However, with some exceptions (Tao et al., 2014), previous studies have primarily focused on  
59 disentangling the relative importance of climate and land use on historical streamflow data. In order to  
60 adequately understand and address the impacts of climate and land use on water resources, tools are  
61 needed to quantify the impacts of these drivers on the complete water cycle (e.g. evapotranspiration [ET],  
62 drainage, and runoff). Furthermore, existing statistical methodologies often implicitly treat land use and  
63 climate effects as step-changes by dividing datasets into two or more discrete time periods (e.g. “before”  
64 and “after”) (Gupta et al., 2015; Li et al., 2009; Tomer & Schilling, 2009; Wang & Hejazi, 2011; Xu et  
65 al., 2013; Zhang et al., 2016). This assumption may be problematic because land use and climate typically  
66 change continuously (and often in tandem with potential interactions), and with gradual hydrological  
67 impacts (Jiang et al., 2015; Marhaento et al., 2017). Therefore, there is a need for improved methods to  
68 separate the impacts of climate and land use in a continuous time series of hydrological data.

69 To meet this challenge, we build upon previous multiple linear regression approaches (Ahn & Merwade,  
70 2014; Huo et al., 2008; Ye et al., 2003) and introduce a new principal components regression-based  
71 method to quantify the impacts of climate and land use change on any measured or modeled hydrological  
72 flux continuously through time. We then apply this new technique to answer the question, to what degree  
73 can land use amplify or counteract climate-induced changes to the water balance of a watershed? Using  
74 both historical data and simulated results from diverse future scenarios for streamflow, ET, drainage, and  
75 direct runoff, we provide insight into the degree to which land use can be used as a local tool to maintain  
76 a watershed within a desired hydrological operating space (Scheffer et al., 2015) in the context of an  
77 uncertain future climate.

## 78 2. Methodology

### 79 2.1 Statistical model description

80 In brief, our new method develops statistical relationships between meteorological variables and any  
81 hydrological flux (HF) of interest during a baseline period. These statistical relationships are then applied  
82 to climate data outside of the baseline period, which we refer to as the prediction period. Predictions are  
83 then used to estimate the changes resulting from climate differences relative to the baseline period at a  
84 monthly resolution, and residuals from predictions are attributed to human activities. By then assessing  
85 the total change from the baseline period relative to the change attributed to human activities, we obtain  
86 the relative importance of land use and climate change continuously through time. A general overview of  
87 the method is presented in Figure 1. While the analysis in this study is done at a monthly timestep  
88 consistent with other regression-based studies separating climate and land use effects (Ahn & Merwade,  
89 2014; Schottler et al., 2014; Xu et al., 2013; Ye et al., 2003; Zhang et al., 2016), the method may be  
90 applied at other time resolutions as long as reliable input data and regression relationships can be  
91 developed.

92 We describe this method for a generic HF in the present section (2.1), and then separately apply it to  
93 historical streamflow data (Section 2.2.1); and simulated future ET, drainage, and direct runoff (Section  
94 2.2.2).

#### 95 2.1.1 Generating baseline relationships

96 To estimate the relative contributions of climate and land use to change in a given HF, a baseline period  
97 must be identified from which relative changes are then calculated. This baseline period should represent  
98 a period of time in which land use is relatively static, so that variability in the HF is driven primarily by  
99 meteorological processes. First, we use significance pruning to select predictor variables for the HF of  
100 interest from a suite of candidate predictor variables within the baseline period at monthly resolution. It is  
101 important that candidate predictor variables are (a) available over the entire period of interest; and (b)  
102 controlled by climate, not land use. In our application (Section 2.2), candidate variables include a variety  
103 of measured and derived meteorological variables (e.g. precipitation, temperature, reference ET). For  
104 each month, candidate predictor variables were mean-centered and scaled to a unit standard deviation to  
105 prevent differences in magnitude or units from affecting statistical relationships. We retain the subset of  
106 candidate predictor variables that have a significant linear relationship with the HF (a significance  
107 threshold of  $p < 0.10$  was used to err on the side of variable retention). Importantly, this approach means  
108 that the retained predictor variables are allowed to differ by each month and HF; for example, incoming  
109 solar radiation may be a more important predictor for ET than direct runoff.

110 To avoid potential overfitting and eliminate collinearity between predictor variables, we transform scaled  
111 variables to principal components (PCs) and use principal components regression (PCR) to predict the HF  
112 of interest. To determine the PCs used for PCR, we use both a variance threshold and significance  
113 pruning approach. PCs explaining a cumulative 80% of total variance in the scaled predictor variables are  
114 selected for PCR, as well as any other PC which has both a significant linear relationship with the HF  
115 ( $p < 0.10$  as above), and explains  $> 1\%$  of total variance in input variables (to avoid spurious correlations).

116 Finally, the selected PCs are used as input to a multiple linear regression equation of the form:

$$\text{HF}_{m,y} = C_0 + C_1 * \text{PC}_{1,m,y} + C_2 * \text{PC}_{2,m,y} + \dots + C_{n,m} * \text{PC}_{n,m,y} + \varepsilon \quad \{\text{Eq. 1}\}$$

117 where  $HF_m$  is the hydrological flux for month  $m$  and year  $y$ ,  $C_x$  are regression coefficients,  $PC_{x,m,y}$  are PCs,  
 118 and  $\varepsilon$  is an error term assumed to be normally distributed and centered on 0. We use a permutation-based,  
 119 split-sample approach to estimate model fit and uncertainty, where the PCR is run 250 times randomly  
 120 sampling 75% of the baseline period for model calibration while retaining 25% for model validation  
 121 (Zipper & Loheide, 2014). This approach provides 250 unique sets of regression coefficients for each  
 122 month and HF.

### 123 2.1.2 Calculating climate and land use contributions to change

124 The statistical relationships for the baseline period are then applied to the rest of the hydrological time  
 125 series (the prediction period). While both of our applications of the method (Section 2.2) have a baseline  
 126 period at the beginning of a hydrological time series, this method can also use modern conditions as the  
 127 baseline period and apply statistical relationships into the past to quantify the relative contribution of  
 128 historical land use and climate change to a given HF. Using the permutation-based approach described  
 129 above, we have 250 estimated values of each HF for each year and month within the prediction period.

130 To separate the relative contribution of climate and land use, we adopt the common assumption that these  
 131 two factors can explain all variability in a given HF relative to the baseline period: climate encompasses  
 132 all changes to drivers from outside the study system (in our case, the watershed), and land use  
 133 encompasses all changes to characteristics internal to the study system (Ahn & Merwade, 2014; Duan et  
 134 al., 2017; Gao et al., 2016; Huo et al., 2008; Jiang et al., 2011). Therefore, changes in land management  
 135 such as irrigation or fertilization practices are included in the land use category.

136 For each HF, we calculate the total change relative to the baseline period ( $\Delta HF_{Total,m,y}$ ) as:

$$\Delta HF_{Total,m,y} = HF_{m,y} - HF_{m,baseline} \quad \{\text{Eq. 2}\}$$

137 where  $HF_{m,y}$  is the measured or modeled hydrological flux for month  $m$  and year  $y$ , and  $HF_{m,baseline}$  is the  
 138 mean HF for that month during the baseline period. The total climate contribution to change  
 139 ( $\Delta HF_{Climate,m,y}$ ) can then be expressed as:

$$\Delta HF_{Climate,m,y} = HF_{PCR,m,y} - HF_{m,baseline} \quad \{\text{Eq. 3}\}$$

140 where  $HF_{PCR,m,y}$  is the PCR-estimated value for month  $m$  and year  $y$ . Finally, the land use component of  
 141 change ( $\Delta HF_{LU,m,y}$ ) is calculated as:

$$\Delta HF_{LU,m,y} = \Delta HF_{Total,m,y} - \Delta HF_{Climate,m,y} = HF_{m,y} - HF_{PCR,m,y} \quad \{\text{Eq. 4}\}$$

142 Note that any of the  $\Delta HF$  variables can be positive or negative, corresponding to an increase/decrease in  
 143 that HF relative to the baseline period. This framework allows us to quantify not just the overall change  
 144 relative to the baseline period for each month, but also under what conditions the effects of land use and  
 145 climate are antagonistic ( $\Delta HF_{LU,m,y}$  and  $\Delta HF_{Climate,m,y}$  have opposite signs) and under what conditions the  
 146 effects of land use and climate are synergistic ( $\Delta HF_{LU,m,y}$  and  $\Delta HF_{Climate,m,y}$  have the same sign).

## 147 2.2 Statistical model application

### 148 2.2.1 Study area

149 We applied the approach described in Section 2.1 to the Yahara River watershed (YW; area=1344 km<sup>2</sup>),  
 150 Wisconsin, USA (Figure 2). The YW is an urbanizing agricultural watershed, and thus is a useful  
 151 analogue for human-influenced watersheds throughout the US Midwest and the world (Carpenter et al.,  
 152 2015b). The water resources of the YW are stressed by various land use and climatic drivers of change  
 153 including (1) an expanding urban core (the city of Madison, Wisconsin's state capital), leading to changes

154 to the water and energy balance (Schatz & Kucharik, 2014; Zipper et al., 2016, 2017b); (2) widespread  
155 fertilized row-crop and dairy agriculture contributing to erosion and nutrient loading (Carpenter et al.,  
156 2015a; Lathrop & Carpenter, 2013; Motew et al., 2017; Qiu & Turner, 2013, 2015); and (3) a long-term  
157 trend of increasing precipitation with more frequent extreme precipitation events in recent decades,  
158 leading to both groundwater and surface water issues (Booth et al., 2016a; Gillon et al., 2016; Usinowicz  
159 et al., 2017). Due to these stresses on the water cycle, improving the understanding and management of  
160 climate and land use effects on water resources is a key goal cutting across hydrological, ecological, and  
161 social research in the YW (Gillon et al., 2016; Motew et al., 2017; Qiu et al., 2017; Wardropper et al.,  
162 2015). We separately investigated the past (Section 2.2.1) and future (Section 2.2.2) of the YW to  
163 quantify how the water cycle of the YW has changed historically and may continue to change under a  
164 variety of scenarios.

165 For clarity, throughout the text the term “discharge” is used to refer to total streamflow as measured at a  
166 gauging station converted to units of depth after dividing by total watershed area; discharge can be  
167 separated into “quickflow” and “baseflow” components (Schwartz & Smith, 2014). “Direct runoff” is  
168 used to refer to overland flow calculated at the grid cell resolution from AgroIBIS output.

### 169 2.2.2 Historical discharge analysis

170 For historical analysis, we focused on the Pheasant Branch subwatershed (PBS; 44.24 km<sup>2</sup>; Figure 2)  
171 which drains the northwest portion of the YW including portions of the municipalities of Madison and  
172 Middleton. We selected the PBS for detailed analysis because it has a relatively long period of discharge  
173 data availability (1974-present). Within this period, there have been well-documented changes in land use  
174 (urbanization, including the connection of former internally-drained basins to the streamflow network),  
175 water governance (stringent infiltration requirements for new developments), climate (increased  
176 precipitation), and flood peaks (increasing discharge) (Gebert et al., 2012). Additionally, the PBS is  
177 upstream of the Yahara chain of lakes (Figure 2), which buffer the impacts of climate on streamflow at  
178 the monthly scale of analysis used here.

179 We applied the PCR relationship using monthly discharge data from the USGS National Water  
180 Information Service gauging station 05427948 (U.S. Geological Survey, 2017) for the period July 1974-  
181 December 2016 (a total of 42 years and 6 months). We defined the baseline period as the first half of the  
182 available streamflow data (July 1974-December 1995; 21 years and 6 months), and the prediction period  
183 as the second half of available discharge data (January 1996-December 2016; 21 years). This breakpoint  
184 also roughly corresponds with an observed shift in historical streamflow beginning in 1993, which has  
185 been attributed to increasing precipitation and urbanization within the PBS (Gebert et al., 2012). The  
186 selection of a suitable baseline period is one of the key user decisions for the method described in Section  
187 2.1.1. To quantify the impacts of the baseline period on results, we also conducted a sensitivity analysis in  
188 which all analyses for the PBS were repeated while varying the end of the baseline period from 1992 to  
189 1998.

190 Predictor variables for the PBS were either measured or derived from the Madison Airport Global  
191 Historical Climatology Network-Daily (GHCN-D) site (USW00014837; 43.14°N, -89.35°E) (Menne et  
192 al., 2012). Directly measured variables were daily precipitation, maximum temperature, and minimum  
193 temperature. Wind speed data was available for only part of the period of interest, and therefore we used  
194 mean values for a given day of year for the entire period. We estimated vapor pressure as the saturation  
195 vapor pressure at minimum daily temperature following Allen et al. (1998). We estimated daily incoming

196 solar radiation using the Bristow-Campbell equation (Bristow & Campbell, 1984), which scales the top-  
197 of-atmosphere solar radiation using an estimated transmissivity based on daily maximum and minimum  
198 temperature, as implemented in the EcoHydRology R package (Fuka et al., 2014). The Bristow-Campbell  
199 equation was calibrated to site conditions using observed incoming shortwave radiation data from the  
200 nearby Arlington Agricultural Research Station (43.31°N, -89.38°E;  
201 [http://agwx.soils.wisc.edu/uwex\\_agwx/awon](http://agwx.soils.wisc.edu/uwex_agwx/awon)) for the period 1986-2016 (Figure S1). We calculated daily  
202 Penman-Monteith reference ET following the UN Food and Agriculture Organization method (Allen et  
203 al., 1998), and precipitation deficit as precipitation – reference ET.

204 We then aggregated daily variables to a monthly set of candidate predictor variables: cumulative monthly  
205 precipitation, reference ET, and precipitation deficit [ $\text{mm mo}^{-1}$ ]; and mean daily minimum and maximum  
206 temperature [ $^{\circ}\text{C}$ ], incoming shortwave solar radiation [ $\text{W m}^{-2}$ ], wind speed [ $\text{m s}^{-1}$ ], relative humidity [%],  
207 actual vapor pressure, saturation vapor pressure, and vapor pressure deficit [kPa]. Candidate predictor  
208 variables included both the month of interest, as well as the month of interest plus the preceding 1, 2, 3, 6,  
209 and 12 months by summing (cumulative variables) or averaging (mean daily variables). We also included  
210 monthly metrics associated with precipitation intensity, including maximum daily precipitation [mm],  
211 total days with precipitation, and total days with precipitation exceeding 12.7, 25.4, 50.8, and 76.2 mm  
212 (0.5", 1", 2", 3"); and metrics allowing for nonlinear responses to precipitation, including squared  
213 monthly precipitation [mm], squared monthly precipitation deficit, and squared cumulative precipitation  
214 deficit for all lags. In total, there were 79 candidate predictor variables evaluated for each month. The  
215 retained variables for each flux are shown in Figure S2.

216 We also performed a parallel set of analyses for the quickflow and baseflow components of discharge in  
217 the PBS separated using a recursive digital filter (Eckhardt, 2005) within the Web-based Hydrography  
218 Analysis Tool (WHAT; Lim et al., 2005). All other analyses were repeated as described above. These  
219 results are presented in the Supplementary Information.

## 220 2.2.3 Future scenario analysis

### 221 2.2.3.1 Biophysical model description

222 To investigate the extent to which climate and land use may impact different components of the water  
223 balance, we simulated a variety of plausible future scenarios for the YW using Agro-IBIS, a gridded,  
224 physically-based dynamic vegetation model including agroecosystems. Agro-IBIS simulates the complete  
225 carbon, energy, and water cycles (Foley et al., 1996; Kucharik et al., 2000; Kucharik, 2003; Kucharik &  
226 Brye, 2003). Recent updates to Agro-IBIS replaced the soil physics with those of HYDRUS-1D (Šimůnek  
227 et al., 2013), so that the soil water balance is solved using the pressure head-based form of the Richards'  
228 Equation (Soylu et al., 2014); added erosion and phosphorus cycling, along with a suite of new land cover  
229 types, for the simulation of the YW (Motew et al., 2017); and coupled Agro-IBIS to MODFLOW to allow  
230 for lateral exchanges of water between Agro-IBIS cells (Zipper et al., 2017a).

231 In this study, we used the version of Agro-IBIS described in Motew et al. (2017), which simulates the  
232 YW at 220-m×220-m spatial resolution. This version of Agro-IBIS is coupled to the streamflow routing  
233 model THMB (Coe, 1998, 2000; Donner & Kucharik, 2003), though THMB output was not used in the  
234 present study. Motew et al. (2017) calibrated and validated the hydrologic performance of the model via  
235 comparison with long-term streamflow records from six USGS gauging stations within the YW.  
236 Sediment/phosphorus transport and soil phosphorus concentrations were also validated against  
237 measurements. Previous validations of Agro-IBIS in the YW include comparisons against plot-scale

238 measurements of soil moisture, soil temperature, leaf area index, aboveground net primary productivity,  
239 drainage, nitrogen cycling, and corn yield (Kucharik & Brye, 2003; Soylu et al., 2014; Zipper et al.,  
240 2015). In the interest of space, the reader is referred to the publications referenced above for additional  
241 information on the structure and validation of Agro-IBIS for the YW.

#### 242 *2.2.3.2 Climate and land use scenarios*

243 Four scenarios, each with a unique climate and land use pathway, were developed to explore alternative  
244 social-political options for human action and socio-economic development in the YW for 2014-2070.  
245 Details of the storylines and biophysical drivers are presented in Carpenter et al. (2015b), Wardropper et  
246 al. (2016), and Booth et al. (2016b). The use of stakeholder-driven qualitative scenarios acknowledges the  
247 many potential paths climate and land use may take in the future, rather than focusing on a single  
248 forecasted future, and allows us to explore the degree to which climate and land use may interact under a  
249 variety of futures (Blöschl & Montanari, 2010).

250 Each of these four scenarios contains a separate set of land use and climate input data (Figure 3), as well  
251 as differences in the crop response to water stress representing agricultural biotechnology improvements.  
252 Full narratives, videos, and other information regarding the scenarios are provided in the above-  
253 referenced publications and at [yahara2070.org](http://yahara2070.org). A brief summary of key land use and climate drivers for  
254 each of the four scenarios follows:

255 **Accelerated Innovation (AI):** AI explores a future in which technology is prioritized as a solution to  
256 climate change. Land use is characterized by expanding urban areas, with a relatively constant  
257 agricultural footprint. Climate change is the least extreme in this scenario, with warming of  $\sim 2^{\circ}\text{C}$  by 2070  
258 and more frequent heavy rainfall events.

259 **Abandonment and Renewal (AR):** AR explores a future in which society is unprepared for climate  
260 change. A mass exodus from the YW leads to a reduction in urban and agricultural land use, and the  
261 landscape primarily returns to natural vegetation. Climate change is the most extreme in this scenario,  
262 with warming of  $5.5^{\circ}\text{C}$  by 2070 and a period of extreme heat waves and floods in the 2030s.

263 **Connected Communities (CC):** CC explores a future in which sustainability and community become  
264 global priorities. Urban land use stays relatively constant, but agricultural land shifts away from row-crop  
265 agriculture to pasture and crops used directly as food (e.g. vegetables and small grains). Climate change  
266 in this scenario is intermediate between AI and AR, with  $3.5^{\circ}\text{C}$  warming by 2070 and both heavy rainfall  
267 and drought becoming more common.

268 **Nested Watersheds (NW):** NW explores a future in which governance is focused around national-scale  
269 water security. Urban land use remains relatively constant, but row-crop agriculture decreases as natural  
270 ecosystems are prioritized for water quality protection. Climate in this scenario is comparable to CC, with  
271  $4^{\circ}\text{C}$  warming by 2070 and more frequent precipitation extremes.

272 We used the PCR approach described in Section 2.1 to evaluate climate and land use impacts on three  
273 HFs: ET, drainage, and direct runoff. These variables were averaged monthly over all non-water grid cells  
274 in the YW based on simulation output from the calibrated Agro-IBIS model of the YW (Motew et al.,  
275 2017). The model was spun-up for 200 years (1786-1985) to equilibrate water, energy, carbon, nitrogen,  
276 and phosphorus cycles using randomly selected meteorological years from the 1986-2013 period. The  
277 1986-2013 period, during which land use and climate were the same for all scenarios, was used as the



278 baseline period. We also ran four additional simulations in which the 2014-2070 future climate scenarios  
279 were simulated with historical land use. Output from these simulations were included in generating the  
280 PCR models in order to prevent statistical extrapolation outside the range of the baseline climate in the  
281 future scenarios, but not included as part of the baseline period when assessing changes through time.

282 For the prediction period (2014-2070), we simulated a factorial combination of all land use and climate  
283 scenarios (16 total simulations) in order to provide a wide range of scenarios to evaluate interactions  
284 between land use and climate change. We used the same meteorological predictor variables as in the  
285 historical streamflow analysis (Section 2.2.2), though in this case they were watershed averages derived  
286 from spatially variable gridded meteorological input datasets (Booth et al., 2016b). The retained variables  
287 for each HF are shown in Figure S3. As in the historical streamflow analysis, we fit the PCR model using  
288 250 randomly sampled permutations of calibration/validation data which divide the baseline period into  
289 75%/25% of available years.

290 For direct comparison with analysis of the PBS, we also extracted modeled monthly direct runoff for the  
291 1974-2016 period from all grid cells within the PBS. For the Agro-IBIS spin-up, which includes 1974-  
292 1985, spatially distributed precipitation data were not available so randomly sampled meteorological  
293 years from the period 1986-2013 were used. For the 2014-2016 period, climate and land use from the AI  
294 scenario were used, though all scenarios are similar during this period. Therefore, we used the 1986-2013  
295 period to compare Agro-IBIS' direct runoff performance for the PBS with quickflow derived from  
296 baseflow separation, and the entire 1974-2016 period for separation of climate and land use effects (with  
297 a 1974-1995 baseline period, as in the historical analysis).

## 298 3. Results

### 299 3.1 Historical discharge analysis

#### 300 3.1.1 Model validation

301 The statistical model fits the observed discharge data for the PBS well, with a monthly root mean squared  
302 error (RMSE) of 6.36 mm (10.8% of the observed range) and an annual RMSE of 21.77 mm (10.9%) for  
303 the validation samples (1974-1995; Figure 4). Nash-Sutcliffe Efficiency (NSE) values indicate that the  
304 model performs acceptably at monthly timesteps and good at annual timesteps (NSE=0.421 and 0.669,  
305 respectively) (Moriassi et al., 2007). When comparing the mean of all validation samples for a given year,  
306 seasonal dynamics are well-captured, though discharge peaks tend to be underestimated (Figure 4a).  
307 However, when considering validation samples from all permutations, it is evident that the PCR method  
308 adequately captures the full range of the observed data and seasonal patterns (Figure 4b).

#### 309 3.1.2 Climate and land use impacts on discharge

310 Within the baseline period (1974-1995), the method forces changes in discharge due to overall, climate,  
311 and land use effects to a mean of 0 mm, as the baseline period is the datum from which changes are  
312 calculated within the prediction period. During the baseline period, there is a slight but not significant  
313 trend in overall changes in discharge and climate-induced changes in discharge of 1.6 mm/yr ( $p>0.05$ ),  
314 and no trend in land use-induced changes (slope=0 mm/yr). This lack of a land use trend during the  
315 baseline period indicates that there is no trend in the residual of the PCR relationships, lending support to  
316 our baseline period selection.

317 Within the prediction period (1996-2016), there is a significant increase in average annual discharge of  
318 57.96 mm ( $p < 0.0001$ ; one-sample t-test) relative to the baseline period (Figure 4). Of the mean overall  
319 change, climate is a slightly stronger contributor than land use, though both have significant impacts.  
320 Climate change causes a mean 34.47 mm increase in discharge ( $p < 0.01$ ; 59.5% of overall change), while  
321 land use change contributes a 23.40 mm increase ( $p < 0.0001$ ; 40.5% of overall change) relative to the  
322 baseline period. However, there is substantial interannual variability in the relative strength of the two  
323 drivers. Overall changes in discharge relative to the baseline period appears to respond most strongly to  
324 climate variability, with a consistent but low-level positive effect due to land use change (Figure 4d).  
325 Land use effects are positive in 19 of 21 years (90%), while climate effects are positive in 16 of 21 years  
326 (76%) (Figure 4e).

327 Quickflow and baseflow contribute approximately equally to the observed increases in annual discharge,  
328 with an overall increase in baseflow of 28.18 mm yr<sup>-1</sup> ( $p < 0.0001$ ; Figure S4) and overall increase in  
329 quickflow of 29.79 mm yr<sup>-1</sup> ( $p < 0.0001$ ; Figure S5). However, the relative contribution of land use and  
330 climate to these two components of overall discharge varies. For quickflow, the increase is dominated by  
331 climate (22.40 mm yr<sup>-1</sup>;  $p < 0.01$ ) with a small but significant contribution from land use (7.38 mm yr<sup>-1</sup>;  
332  $p = 0.03$ ). In contrast, for baseflow the increase due to land use is larger (15.50 mm yr<sup>-1</sup>;  $p < 0.0001$ ) than  
333 the increase due to climate (12.67 mm yr<sup>-1</sup>;  $p < 0.001$ ); however, the proportion of total change in baseflow  
334 attributed to land use may be an overestimate due to long timescales of baseflow response to changes in  
335 watershed-scale subsurface storage (see Section 4.1).

336 Using our continuous PCR-based approach, we also identify changes through time in the relative  
337 contribution of climate and land use. While discharge is increasing through time at a rate of 2.97 mm yr<sup>-1</sup>,  
338 this trend is not significant ( $p = 0.07$ ). However, land use effects are significantly increasing through time  
339 (1.89 mm yr<sup>-1</sup>;  $p = 0.02$ ), while climate effects are relatively static ( $p = 0.52$ ). This corresponds with a  
340 significant positive trend in the percent of the watershed with urban land use (1.18 %/year;  $p < 0.05$ ). The  
341 trend in discharge is primarily driven by increases in baseflow, which has positive overall (1.80 mm/yr;  
342  $p = 0.02$ ) and land use trends (1.33 mm yr<sup>-1</sup>;  $p < 0.01$ ) with no significant climate trend ( $p = 0.38$ ) during the  
343 prediction period (Figure S4). In contrast, there are no significant quickflow trends for overall, land use,  
344 or climate changes (Figure S5).

### 345 3.1.3 Sensitivity analysis of baseline period

346 While the results described above all use a baseline period of 1974-1995, model performance is  
347 comparable regardless of the baseline period used as long as the baseline period includes 1993, a  
348 particularly high flow year (Figure 5a). Similarly, the relative importance of land use and climate are  
349 comparable for all baseline periods ending in 1993 or later at both a mean and interannual scale.  
350 Comparing within the common prediction period (1999-2016), the only significant differences in PCR-  
351 estimated changes due to land use between baseline period end years are a significant difference between  
352 1992 and 1996-1998 (Figure 5b). For changes due to climate, there are no significant differences between  
353 any of the baseline period end years (Figure 5c).

## 354 3.2 Future scenario analysis

### 355 3.2.1 Model validation

356 When analyzing output from the simulated future scenarios, monthly PCR models perform very well,  
357 with NSE of 0.982, 0.793, and 0.920 for ET, drainage, and direct runoff, respectively (Figure 6). RMSE

358 are 5.14 mm (3.87% of range of observations), 5.84 mm (5.84%), and 5.07 mm (1.84 %), respectively.  
359 Performance is also strong at an annual level, with NSE of 0.786, 0.914, and 0.911 for ET, drainage, and  
360 direct runoff. Statistics summarizing overall and monthly fits for each hydrological flux are provided in  
361 Table S1.

### 362 3.2.2 Climate and land use impacts on the water balance

363 The scenarios generated a wide range of climate and land use model inputs that exposed the relative  
364 impacts of these two drivers under a variety of conditions, with AI and AR representing the extremes for  
365 most inputs (Figure 3). For example, while air temperature increased in all scenarios relative to the  
366 historical period, there is  $\sim 4^{\circ}\text{C}$  difference across the four scenarios, with the most extreme increase in AR  
367 and the mildest increase in AI. Similarly, precipitation changes varied across the four scenarios, with  
368  $\sim 400$  mm of variability between scenarios; AR had the most extreme increases in precipitation,  
369 particularly during the 2030s. Land use change also varied substantially between scenarios; row-crop  
370 agriculture, for example, was relatively consistent through time in the AI scenario, but decreased in each  
371 of the other scenarios and was almost completely eliminated by the end of the AR scenario. Urban land  
372 use was highest for the AI scenario, lowest in the AR scenario, and relatively unaffected in the CC and  
373 NW scenarios.

374 Changes in watershed-average ET are uniformly positive relative to the baseline period across all  
375 combinations of scenarios, ranging from  $23.42 \text{ mm yr}^{-1}$  to  $90.76 \text{ mm yr}^{-1}$  over the final two decades of the  
376 simulations (Figures 7a, 8a). These increases are dominated by climate effects ( $42.29 \text{ mm yr}^{-1}$  to  $91.95$   
377  $\text{mm yr}^{-1}$ ), with a small but antagonistic effect of land use ( $-19.53 \text{ mm yr}^{-1}$  to  $-1.16 \text{ mm yr}^{-1}$ ). The effects of  
378 land use tend to most strongly counteract those of climate in the AR scenario, which is characterized by  
379 decreases in row-crop agriculture and increases in natural vegetation, while land use effects are closest to  
380 0 in the AI scenario, which is characterized by widespread expansion of impervious cover. Patterns in ET  
381 through time correspond primarily to changes in temperature and reference ET. For example, in all  
382 scenarios with AI climate ET peaks in the 2040s, declines through the 2050s to a low in  $\sim 2060$ , and rises  
383 in the final decade of the simulations (Figure 7a); this pattern corresponds with temperature in the AI  
384 scenario, which is one of the primary controls on reference ET (Figure 3).

385 There is more temporal variability in drainage results compared to ET, with overall mean changes ranging  
386 from  $-142.12 \text{ mm yr}^{-1}$  to  $65.17 \text{ mm yr}^{-1}$  over the final two decades of the simulations (Figures 7b, 8b).  
387 Both climate and land use can have positive effects (increase in drainage) and negative effects (decrease  
388 in drainage), though as with ET the effects of climate are dominant. Climate effects range from  $-124.85$   
389  $\text{mm yr}^{-1}$  to  $41.76 \text{ mm yr}^{-1}$ , and land use effects from  $-17.33 \text{ mm yr}^{-1}$  to  $28.08 \text{ mm yr}^{-1}$ . Unlike ET,  
390 however, climate-driven and land use-driven do not have a consistent synergistic or antagonistic  
391 character, with a synergistic interaction in the AI, CC and NW climate scenarios and an antagonistic  
392 interaction in the AR climate scenario (Figure 8b). However, this directional change is not constant  
393 through time. Across all scenarios with AR land use, in particular with AI and AR climate, the effects of  
394 land use on drainage are positive in the 2040s and 2050s (Figure 7b), a period characterized by a decrease  
395 in urban land use and increase in natural vegetation (Figure 3). While ET seems to be driven primarily by  
396 temperature, changes in drainage respond more to the relative balance of ET and precipitation. In the AR  
397 climate scenario, changes in drainage relative to the baseline period begin declining from their peak in the  
398 late 2040s, becoming negative in the mid-2050s and plateauing in around 2060 for the remainder of the

399 simulation. This trend coincides with a period of decreasing precipitation and increasing reference ET  
400 (Figure 3).

401 Like ET, direct runoff increases in all future scenarios, with increases ranging from 8.27 mm yr<sup>-1</sup> to 49.42  
402 mm yr<sup>-1</sup> over the final two decades of the scenarios (Figures 7c, 8c). As with ET, the effects of climate  
403 tend to dominate with land use effects mostly contributing to a small but antagonistic effect: climate  
404 accounts for 9.08 mm yr<sup>-1</sup> to 53.86 mm yr<sup>-1</sup> of overall changes, compared to -5.76 mm yr<sup>-1</sup> to +0.02 mm  
405 yr<sup>-1</sup> for land use. Through time, changes in direct runoff track total annual precipitation, annual extreme  
406 precipitation events, and annual reference ET (Figure 3a,b,d). For example, in the AR climate scenarios,  
407 changes in direct runoff are largest in the 2030s and 2040s (Figure 7c), the wettest period on record which  
408 included the largest number of extreme precipitation days (Figure 3). In contrast, the NW climate  
409 scenarios have a decline in direct runoff from the 2040s through the end of the simulation (Figure 7c)  
410 which occurs despite increasing overall and extreme precipitation due to increasing temperature and  
411 reference ET (Figure 3).

## 412 4. Discussion

### 413 4.1 Historical changes in discharge

414 Our results for the PBS indicate that land use contributes to ~40% of observed increases in discharge  
415 while climate contributes ~60%, a trend of unknown origin previously documented by Gebert et al.  
416 (2012). However, while these contributions are comparable, our method's ability to provide continuous  
417 results through time provides insight into the changing relative importance of these two drivers: land use-  
418 induced changes in discharge are increasing through time at approximately twice the rate of climate-  
419 driven changes. This trend appears to be driven primarily by a strong trend of increasing urban land  
420 cover, with a land use-driven increase in discharge of 1.60 mm for each 1% increase in urban land use  
421 within the PBS.

422 Disentangling these two drivers, as well as their changes through time, provides insight into potential  
423 effects of historical watershed-scale management decisions. While urbanization-driven increases in  
424 discharge are often associated with the largest increases during the most extreme events (Boggs & Sun,  
425 2011; Rose & Peters, 2001), our results indicate that at the monthly scale increases in quickflow and  
426 baseflow are comparable (our analysis is done at a monthly timestep and is not intended to capture effects  
427 at the event scale). Moreover, overall and land use effects on baseflow are increasing through time, unlike  
428 quickflow.

429 Given that the period of study coincides with an expansion of urban and impervious cover, the significant  
430 effect of land use change on baseflow, not quickflow, is surprising. While outside the scope of the present  
431 study, we suggest two possible explanations for this result which may be operating in tandem. First, the  
432 observed increase in baseflow may demonstrate that strict infiltration requirements for new developments  
433 in the PBS (Ch. 26.06(3), City of Middleton ordinances) are successfully reducing the impacts of climate  
434 change and urbanization on direct runoff, but are increasing groundwater recharge and baseflow due to  
435 more focused infiltration as well as other potential water sources associated with urbanization (e.g. urban  
436 irrigation). Second, our PCR-based methodology may be attributing the effects of long-term increases in  
437 groundwater storage to land use change. There is a long-term increasing trend in groundwater levels of  
438 0.3 m decade<sup>-1</sup> with substantial variability at yearly to decadal timescales and a nonlinear response of  
439 baseflow to water table depth (Figure S8). Since changes in storage are endogenous to the PBS and the

440 timescale over which groundwater storage changes are longer than the maximum timescale considered in  
441 our PCR relationships (one year), baseflow response to changes in watershed-scale storage could be  
442 methodologically attributed to the effects of land use change, which tends to follow long-term trends but  
443 has little interannual variability.

444 Combined, these results may help guide future management interventions targeted at buffering the  
445 observed changes in discharge, quickflow, and baseflow associated with urbanization. Infiltration-based  
446 stormwater management (e.g. distributed green infrastructure) may have an unintended effect of  
447 increasing baseflow, potentially creating more drought-resistant streams. Given that infiltration-based  
448 stormwater management is also effective at counteracting climate-induced changes in discharge during  
449 extreme events, these practices may present an opportunity to protect aquatic ecosystems during both  
450 low- and high-flow periods, though work elsewhere has found that reductions in runoff volumes do not  
451 always translate to increased baseflow due to watershed-specific factors such as the amount and  
452 distribution of impervious cover (Fanelli et al., 2017). This highlights a need to better understand how  
453 land use propagates through groundwater flow systems to impact downstream terrestrial and aquatic  
454 ecosystems (Bhaskar et al., 2016; Jefferson et al., 2017; Zipper et al., 2017a).

#### 455 4.2 Future scenario analysis

456 Results from our factorial set of scenarios indicate that the effects of climate, not land use change, will  
457 likely dominate the future water balance of the YW. Specifically, ET seems to respond most strongly to  
458 temperature, while direct runoff responds most strongly to precipitation. Climate effects on drainage are  
459 driven primarily by the balance of supply (precipitation) and demand (reference ET). As precipitation  
460 projections have considerably less certainty than temperature projections (WICCI, 2011), this makes  
461 understanding the impacts of climate and land use change on surface water and groundwater resources  
462 particularly challenging. In fact, the similarity of predicted land use effects between different land use  
463 scenarios for a given climate (e.g. columns in Figures 7 and 8) indicates that the effects of land use  
464 change may be smaller than errors in the PCR relationships.

465 While the effects of land use are smaller than those of climate, several key patterns and interactions with  
466 climate emerge. Fluxes occurring at the land surface (ET and direct runoff) tend to have antagonistic  
467 relationships between climate and land use effects, with increases resulting from climate change partially  
468 counteracted by decreases resulting from land use effects. This indicates that, while the effects are  
469 relatively small, land use changes can act as a buffer from climate change at a watershed scale. In  
470 contrast, drainage has a mix of synergistic and antagonistic effects and the largest land use effects of any  
471 of the fluxes studied, exceeding 50% of overall change in some combinations of land use and climate  
472 scenarios. While groundwater recharge is typically thought of as beneficial, excess groundwater can have  
473 negative effects on several ecosystem services including reductions in flood retention capabilities, risk of  
474 basement flooding in urban areas, and decreases in agricultural productivity associated with oxygen stress  
475 (Booth et al., 2016a). It is therefore critical to consider the implications of either an increase or decrease  
476 in watershed-scale drainage for groundwater flow and associated ecosystems when making land use  
477 decisions.

478 Additionally, the AI land use scenario (characterized by urbanization) and AR land use scenario  
479 (characterized by a return to natural ecosystems) consistently have the most extreme impacts on the water  
480 balance. Across all scenarios, AI has the smallest effect on ET and drainage, but the largest effect (most  
481 negative) on direct runoff. In contrast, AR has the largest effect on drainage (most positive) and ET (most

482 negative), and among the smallest effects on direct runoff. This highlights the important role of land use  
483 in determining the partitioning of water at the land surface and in the root zone.

#### 484 4.3 Synthesis and management implications

485 Both the historical discharge analysis in the PBS and the future scenario analysis of the YW indicate that  
486 climate is the key control over the water balance, though the analyses differ in the relative importance of  
487 land use. In the PBS, results indicate that climate change contributes to ~60% of observed changes in  
488 discharge, with approximately equal impacts on quickflow and baseflow, though the effects of land use  
489 are increasing through time. In contrast, the simulated future scenario analysis points to climate as the key  
490 control over direct runoff (as well as ET and drainage), with relatively smaller effects of land use. To  
491 better assess potential causes of these differences, we extracted Agro-IBIS direct runoff output from the  
492 Pheasant Branch portion of the YW and repeated all analyses for the common period of record (1974-  
493 2016). While the baseline period data differs between the two analyses due to different meteorological  
494 input data in the 1974-1985 period (see section 2.2.3.2), results for the overall degree of change are  
495 comparable. Results from historical analysis of the Agro-IBIS output for Pheasant Branch (Figure S6)  
496 finds that 59.4% of the overall changes in direct runoff during the prediction period result from climate  
497 and 40.6% result from land use (compared to 75.2% climate and 24.8% land use for quickflow estimated  
498 from baseflow separation; Figure S5). Also similar to the results from baseflow separation, there is no  
499 significant trend through time for overall, land use, or climate-induced changes in Agro-IBIS direct runoff  
500 for the portion of the prediction period with real climate inputs (1996-2013).

501 This analysis indicates that the differences between the historical discharge analysis and the future  
502 scenario analysis is driven by several factors. First, the degree and trajectory of land use change varies  
503 between the spatial scales used for the two analyses. The PBS is significantly smaller than the YW (~3%  
504 of the YW) and has experienced relatively monodirectional land use change (urbanization) during the  
505 historical period (Figure 4c). In contrast, the future scenarios include a large variety of contrasting land  
506 use changes which may partially counteract each other when aggregated to the watershed scale. The  
507 stronger land use signal in the PBS relative to the YW implies that, just as the impacts of climate change  
508 on streamflow are attenuated in larger river networks (Chezik et al., 2017), so too can larger spatial scales  
509 attenuate the effects of land use change. Second, climate change during the future scenario analysis (2°C  
510 to 5.5°C warming) is more extreme than has been observed in the historical record. Third, our modelling  
511 approach may underestimate differences in hydrological properties between land uses (see Section 4.4).

512 While our analysis agrees with recent work showing that climate effects may dominate future  
513 hydrological changes (Martin et al., 2017; Peng et al., 2016; Pribulick et al., 2016; Wang et al., 2017), we  
514 also highlight the critical need to target land use interventions locally to maximize benefits in areas of  
515 concern (Fry & Maxwell, 2017). The results presented for the YW average hydrologic response over an  
516 area of 1344 km<sup>2</sup>, and therefore neglect spatial heterogeneity in land use which can impact the local water  
517 cycle (Deshmukh & Singh, 2016; Fanelli et al., 2017; Frans et al., 2013; Haddeland et al., 2007). As  
518 observed in the historical discharge analysis, management interventions can impact hydrological  
519 processes at a comparable level to climate change, in the case of the PBS by increasing the baseflow  
520 contribution to changes in streamflow through time via stormwater management and infiltration  
521 requirements in new land developments.

522 Elsewhere, previous work has shown that, for example, the expansion of biofuel cropping systems can  
523 change ET (Harding et al., 2016; Joo et al., 2017; VanLoocke et al., 2010; Wagner et al., 2017); land use

524 change can either reduce or increase groundwater recharge (Giménez et al., 2016; Newcomer et al., 2014;  
525 Oliveira et al., 2017; Qiu & Turner, 2015; Robertson et al., 2017; Zipper et al., 2017a); and urban green  
526 infrastructure and agricultural drainage management can successfully reduce runoff volumes (Allred et  
527 al., 2003; Elliott et al., 2016; Schott et al., 2017; Shuster et al., 2017; Wadzuk et al., 2010). Each of these  
528 represents a management practice that can alter a hydrologic flux of interest in the context of climate  
529 change which may have significant local benefits.

#### 530 4.4 Methodological strengths and limitations

531 While statistical regression techniques have previously been used to separate the impacts of climate and  
532 land use on streamflow (Section 2.1), our technique has several novel contributions. First, users of  
533 regression-based methods typically divide their data into two discrete chunks (“before” and “after”) and  
534 separate the temporally-averaged land use and climate impacts using residuals from the “after” period. In  
535 reality, of course, both land use and climate change are rarely step changes, but rather shift gradually over  
536 time. While the approach introduced here uses a baseline period, it also provides continuous estimates of  
537 the relative importance of land use and climate change over time during both the baseline and prediction  
538 period, which makes it possible to identify trends in drivers of hydrological change. For example, in the  
539 PBS, we reveal that the impacts of land use change are increasing over time for both discharge and  
540 baseflow; while climate change has significantly increased streamflow but there is no significant trend  
541 during the prediction period. Second, the continuous separation through time makes it possible to assess  
542 synergistic and antagonistic relationships between climate and land use, as well as the changing nature of  
543 these interactions through time. Third, as opposed to multiple linear regression used elsewhere (Huo et  
544 al., 2008; Jiang et al., 2011; Ye et al., 2003; Zhang et al., 2016), we use a principal components regression  
545 (PCR) approach which transforms input data to maximize orthogonality. Our PCR approach relies on  
546 automated significance-pruning to select predictor variables from a set of candidates, thus reducing  
547 potential spurious correlations and potential researcher biases and providing more robust predictions  
548 (Tang & Wang, 2017; Zimmerman et al., 2016).

549 We do, however, note several potential limitations to our method. For instance, developing statistical  
550 relationships based on one period of time and applying them to another may result in extrapolation  
551 beyond the conditions for which the relationships are well-suited. This problem is common to all  
552 regression-based methodologies and may be particularly challenging in the context of nonstationarity or  
553 where emergent properties of the relationship between climate and land use change lead to novel future  
554 responses (Milly et al., 2008), or where significant changes in watershed storage occur (e.g. rising  
555 groundwater levels as discussed in Section 4.1). In our case, sensitivity analysis results demonstrate that  
556 separation of climate and land use effects is relatively insensitive to the selection of the baseline period, as  
557 long as the performance of the PCR model is validated and demonstrated to accurately reproduce  
558 observations, thus minimizing concerns regarding nonstationarity. We find that results are statistically  
559 identical for baseline periods which include the year 1993, which seems to be particularly important for  
560 including in the baseline period due to the high discharge observed in that year (Figure 4). PCR models  
561 which do not include 1993 in the baseline period tend to underpredict discharge during high flow years  
562 (Figure 5). This implies that care should be taken when selecting the baseline period to ensure that the  
563 meteorological data is representative of the entire period of record, for example by evaluating interannual  
564 variability in the predictor variables during the baseline period relative to the prediction period, to avoid  
565 extrapolating beyond the calibration range. The split-sample validation technique used in this study

566 adequately captures this risk by quantifying a significantly lower NSE when the baseline period does not  
567 include 1993 (Figure 5).

568 Furthermore, while Agro-IBIS is a state-of-the-art dynamic vegetation and agroecosystem model, some  
569 land use characteristics which may impact the water cycle are not represented. For example, changes in  
570 soil hydraulic properties between land uses and through time are not simulated (Paturel et al., 2017), nor  
571 are soil hydraulic properties coupled to soil organic content (Ankenbauer & Loheide, 2017). Improving  
572 parameterizations and including these processes would likely increase the simulated differences between  
573 land use types in the future scenario analysis and increase the relative importance of land use. Our  
574 statistical relationships also do not take into account other factors which may drive changes in the water  
575 balance; for example, each scenario has a representative atmospheric CO<sub>2</sub> concentration pathway (Booth  
576 et al., 2016b). Given that carbon and water cycles are coupled in Agro-IBIS via stomatal conductance,  
577 CO<sub>2</sub> may also be a relevant predictor variable, particularly for ET and under conditions with significant  
578 land use change between C3 to C4 vegetation (Twine et al., 2013). However, in order to make our  
579 methodology broadly applicable to easily obtained meteorological data, we elected to exclude CO<sub>2</sub> and  
580 other non-meteorological predictors from analysis.

## 581 5. Conclusions

582 This study introduces a new principal components regression-based approach to separate the effects of  
583 climate and land use on the water cycle continuously through time, and applies the approach to both  
584 observed and modeled data for the YW in south-central Wisconsin. Analysis of historical discharge data  
585 for the PBS indicates that climate change has caused ~60% of the observed changes in discharge over the  
586 past two decades, with a significantly increasing impact of land use change (urbanization) on both  
587 baseflow and overall discharge. Using a factorial combination of four contrasting land use and climate  
588 scenarios, we find that future changes in the YW's land surface water balance (ET, drainage, and direct  
589 runoff) are likely to be dominated by effects of climate change: ET is most affected by changes in  
590 temperature, direct runoff by changes in precipitation, and drainage by changes in both precipitation and  
591 reference ET. Land use effects are larger on drainage than either ET or direct runoff.

592 Overall, these results indicate that the effects of land use and climate are not static through time, and  
593 separating the relative contribution of these two variables to hydrological change should not be done via  
594 the simple separation of time into discrete elements; rather, it must be done in a continuous manner.  
595 Furthermore, we show that using land use to mitigate the effects of climate change on the water cycle  
596 may be challenging in large watersheds which contain a diversity of land use trajectories. However, our  
597 results indicate that the effects of land use change are larger in the PBS than the YW as a whole due to the  
598 relatively monodirectional land use change from agriculture to urbanization. Therefore, local management  
599 interventions targeted at subwatershed scales to achieve specific desired outcomes may be an effective  
600 path forward to protecting water resources from future climate change.

## 601 6. Acknowledgments

602 This research was funded by the National Science Foundation Water Sustainability & Climate program  
603 (DEB-1038759) and Long-Term Ecological Research Program (DEB-0822700). All statistical analyses  
604 were performed using R v3.4.0 (R Core Team, 2017) and graphics made using ggplot2 (Wickham, 2009)  
605 and InkScape (The Inkscape Team, 2015). Data and code are available on GitHub at  
606 [http://www.github.com/szipper/WaterBalance\\_ClimateVsLULC](http://www.github.com/szipper/WaterBalance_ClimateVsLULC).



## 607 7. References

- 608 Ahn, K.-H., & Merwade, V. (2014). Quantifying the relative impact of climate and human activities on  
609 streamflow. *Journal of Hydrology*, 515, 257–266. <https://doi.org/10.1016/j.jhydrol.2014.04.062>
- 610 Allen, R. G., Pereira, L. S., Raes, D., & Smith, M. (1998). *Crop evapotranspiration: Guidelines for*  
611 *computing crop water requirements* (FAO Irrigation and Drainage Paper No. 56). Rome: United  
612 Nations Food and Agriculture Organization. Retrieved from  
613 <http://www.kimberly.uidaho.edu/water/fao56/fao56.pdf>
- 614 Allred, B. J., Brown, L. C., Fausey, N. R., Cooper, R. L., Clevenger, W. B., Prill, G. L., ... Czartoski, B.  
615 J. (2003). Water table management to enhance crop yields in a Wetland Reservoir Subirrigation  
616 System. *Applied Engineering in Agriculture*, 19(4), 407–421.
- 617 Ankenbauer, K. J., & Loheide, S. P. (2017). The effects of soil organic matter on soil water retention and  
618 plant water use in a meadow of the Sierra Nevada, CA. *Hydrological Processes*, 31(4), 891–901.  
619 <https://doi.org/10.1002/hyp.11070>
- 620 Bhaskar, A. S., Jantz, C., Welty, C., Drzyzga, S. A., & Miller, A. J. (2016). Coupling of the Water Cycle  
621 with Patterns of Urban Growth in the Baltimore Metropolitan Region, United States. *JAWRA*  
622 *Journal of the American Water Resources Association*, 52(6), 1509–1523.  
623 <https://doi.org/10.1111/1752-1688.12479>
- 624 Blöschl, G., & Montanari, A. (2010). Climate change impacts—throwing the dice? *Hydrological*  
625 *Processes*, 24(3), 374–381. <https://doi.org/10.1002/hyp.7574>
- 626 Boggs, J. L., & Sun, G. (2011). Urbanization alters watershed hydrology in the Piedmont of North  
627 Carolina. *Ecology*, 92(2), 256–264. <https://doi.org/10.1002/eco.198>
- 628 Booth, E. G., Zipper, S. C., Loheide, S. P., & Kucharik, C. J. (2016a). Is groundwater recharge always  
629 serving us well? Water supply provisioning, crop production, and flood attenuation in conflict in  
630 Wisconsin, USA. *Ecosystem Services*, 21, Part A, 153–165.  
631 <https://doi.org/10.1016/j.ecoser.2016.08.007>
- 632 Booth, E. G., Qiu, J., Carpenter, S. R., Schatz, J., Chen, X., Kucharik, C. J., ... Turner, M. G. (2016b).  
633 From qualitative to quantitative environmental scenarios: Translating storylines into biophysical  
634 modeling inputs at the watershed scale. *Environmental Modelling & Software*, 85, 80–97.  
635 <https://doi.org/10.1016/j.envsoft.2016.08.008>
- 636 Bristow, K. L., & Campbell, G. S. (1984). On the relationship between incoming solar radiation and daily  
637 maximum and minimum temperature. *Agricultural and Forest Meteorology*, 31(2), 159–166.  
638 [https://doi.org/10.1016/0168-1923\(84\)90017-0](https://doi.org/10.1016/0168-1923(84)90017-0)
- 639 Carpenter, S. R., Booth, E. G., Kucharik, C. J., & Lathrop, R. C. (2015a). Extreme daily loads: role in  
640 annual phosphorus input to a north temperate lake. *Aquatic Sciences*, 77(1), 71–79.  
641 <https://doi.org/10.1007/s00027-014-0364-5>
- 642 Carpenter, S. R., Booth, E. G., Gillon, S., Kucharik, C. J., Loheide, S., Mase, A. S., ... Wardropper, C. B.  
643 (2015b). Plausible futures of a social-ecological system: Yahara watershed, Wisconsin, USA.  
644 *Ecology and Society*, 20(2), 10. <https://doi.org/10.5751/ES-07433-200210>
- 645 Chawla, I., & Mujumdar, P. P. (2015). Isolating the impacts of land use and climate change on  
646 streamflow. *Hydrology and Earth System Sciences*, 19(8), 3633–3651.  
647 <https://doi.org/10.5194/hess-19-3633-2015>
- 648 Chezik, K. A., Anderson, S. C., & Moore, J. W. (2017). River networks dampen long-term hydrological  
649 signals of climate change. *Geophysical Research Letters*, 44(14), 2017GL074376.  
650 <https://doi.org/10.1002/2017GL074376>

651 Coe, M. T. (1998). A linked global model of terrestrial hydrologic processes: Simulation of modern  
652 rivers, lakes, and wetlands. *Journal of Geophysical Research: Atmospheres*, 103(D8), 8885–  
653 8899. <https://doi.org/10.1029/98JD00347>

654 Coe, M. T. (2000). Modeling Terrestrial Hydrological Systems at the Continental Scale: Testing the  
655 Accuracy of an Atmospheric GCM. *Journal of Climate*, 13(4), 686–704.  
656 [https://doi.org/10.1175/1520-0442\(2000\)013<0686:MTHSAT>2.0.CO;2](https://doi.org/10.1175/1520-0442(2000)013<0686:MTHSAT>2.0.CO;2)

657 Deshmukh, A., & Singh, R. (2016). Physio-climatic controls on vulnerability of watersheds to climate  
658 and land use change across the U. S. *Water Resources Research*, 52(11), 8775–8793.  
659 <https://doi.org/10.1002/2016WR019189>

660 Donner, S. D., & Kucharik, C. J. (2003). Evaluating the impacts of land management and climate  
661 variability on crop production and nitrate export across the Upper Mississippi Basin. *Global*  
662 *Biogeochemical Cycles*, 17(3), 1085. <https://doi.org/10.1029/2001GB001808>

663 Duan, L., Man, X., Kurylyk, B. L., Cai, T., & Li, Q. (2017). Distinguishing streamflow trends caused by  
664 changes in climate, forest cover, and permafrost in a large watershed in northeastern China.  
665 *Hydrological Processes*, 31(10), 1938–1951. <https://doi.org/10.1002/hyp.11160>

666 Eckhardt, K. (2005). How to construct recursive digital filters for baseflow separation. *Hydrological*  
667 *Processes*, 19(2), 507–515. <https://doi.org/10.1002/hyp.5675>

668 Elliott, R. M., Gibson, R. A., Carson, T. B., Marasco, D. E., Culligan, P. J., & McGillis, W. R. (2016).  
669 Green roof seasonal variation: comparison of the hydrologic behavior of a thick and a thin  
670 extensive system in New York City. *Environmental Research Letters*, 11(7), 074020.  
671 <https://doi.org/10.1088/1748-9326/11/7/074020>

672 Fanelli, R., Prestegard, K., & Palmer, M. (2017). Evaluation of infiltration-based stormwater  
673 management to restore hydrological processes in urban headwater streams. *Hydrological*  
674 *Processes*, 31(19), 3306–3319. <https://doi.org/10.1002/hyp.11266>

675 Foley, J. A. (2005). Global consequences of land use. *Science*, 309(5734), 570–574.  
676 <https://doi.org/10.1126/science.1111772>

677 Foley, J. A., Prentice, I. C., Ramankutty, N., Levis, S., Pollard, D., Sitch, S., & Haxeltine, A. (1996). An  
678 integrated biosphere model of land surface processes, terrestrial carbon balance, and vegetation  
679 dynamics. *Global Biogeochemical Cycles*, 10(4), 603–628. <https://doi.org/10.1029/96GB02692>

680 Frans, C., Istanbuloglu, E., Mishra, V., Munoz-Arriola, F., & Lettenmaier, D. P. (2013). Are climatic or  
681 land cover changes the dominant cause of runoff trends in the Upper Mississippi River Basin?  
682 *Geophysical Research Letters*, 40(6), 1104–1110. <https://doi.org/10.1002/grl.50262>

683 Fry, J. A., Xian, G., Jin, S. M., Dewitz, J. A., Homer, C. G., Yang, L. M., ... Wickham, J. D. (2011).  
684 Completion of the 2006 National Land Cover Database for the conterminous United States.  
685 *PE&RS, Photogrammetric Engineering & Remote Sensing*, 77(9), 858–864.

686 Fry, T. J., & Maxwell, R. M. (2017). Evaluation of distributed BMPs in an urban watershed—High  
687 resolution modeling for stormwater management. *Hydrological Processes*, 31(15), 2700–2712.  
688 <https://doi.org/10.1002/hyp.11177>

689 Fuka, D., Walter, M., Archibald, J., Steenhuis, J., & Easton, Z. (2014). EcoHydRology: A community  
690 modeling foundation for Eco-Hydrology (Version 0.4.12). Retrieved from [https://CRAN.R-](https://CRAN.R-project.org/package=EcoHydRology)  
691 [project.org/package=EcoHydRology](https://CRAN.R-project.org/package=EcoHydRology)

692 Gao, Z., Zhang, L., Zhang, X., Cheng, L., Potter, N., Cowan, T., & Cai, W. (2016). Long-term  
693 streamflow trends in the middle reaches of the Yellow River Basin: detecting drivers of change.  
694 *Hydrological Processes*, 30(9), 1315–1329. <https://doi.org/10.1002/hyp.10704>

695 Gebert, W. A., Rose, W. J., & Garn, H. S. (2012). *Evaluation of the Effects of City of Middleton*  
696 *Stormwater-Management Practices on Streamflow and Water-Quality Characteristics of*  
697 *Pheasant Branch, Dane County, Wisconsin, 1975-2008* (No. Scientific Investigations Report  
698 2012–5014) (p. 27). Middleton WI: U.S. Geological Survey. Retrieved from  
699 <https://pubs.usgs.gov/sir/2012/5014/>

700 Gillon, S., Booth, E. G., & Rissman, A. R. (2016). Shifting drivers and static baselines in environmental  
701 governance: challenges for improving and proving water quality outcomes. *Regional*  
702 *Environmental Change*, 16(3), 759–775. <https://doi.org/10.1007/s10113-015-0787-0>

703 Giménez, R., Mercau, J., Noretto, M., Páez, R., & Jobbágy, E. (2016). The ecohydrological imprint of  
704 deforestation in the semiarid Chaco: insights from the last forest remnants of a highly cultivated  
705 landscape. *Hydrological Processes*, 30(15), 2603–2616. <https://doi.org/10.1002/hyp.10901>

706 Gupta, S. C., Kessler, A. C., Brown, M. K., & Zvomuya, F. (2015). Climate and agricultural land use  
707 change impacts on streamflow in the upper midwestern United States. *Water Resources Research*,  
708 51(7), 5301–5317. <https://doi.org/10.1002/2015WR017323>

709 Gyawali, R., Greb, S., & Block, P. (2015). Temporal changes in streamflow and attribution of changes to  
710 climate and landuse in Wisconsin watersheds. *JAWRA Journal of the American Water Resources*  
711 *Association*, 51(4), 1138–1152. <https://doi.org/10.1111/jawr.12290>

712 Haddeland, I., Skaugen, T., & Lettenmaier, D. P. (2007). Hydrologic effects of land and water  
713 management in North America and Asia: 1700-1992. *Hydrology and Earth System Sciences*,  
714 11(2), 1035–1045.

715 Harding, K. J., Twine, T. E., VanLoocke, A., Bagley, J. E., & Hill, J. (2016). Impacts of second-  
716 generation biofuel feedstock production in the central U.S. on the hydrologic cycle and global  
717 warming mitigation potential. *Geophysical Research Letters*, 43(20), 2016GL069981.  
718 <https://doi.org/10.1002/2016GL069981>

719 Homer, C., Dewitz, J., Yang, L., Jin, S., Danielson, P., Xian, G., ... Megown, K. (2015). Completion of  
720 the 2011 National Land Cover Database for the conterminous United States - Representing a  
721 decade of land cover change information. *Photogrammetric Engineering and Remote Sensing*,  
722 81(5), 345–354. <https://doi.org/10.14358/PERS.81.5.345>

723 Homer, C., Dewitz, J., Fry, J., Coan, M., Hossain, N., Larson, C., ... Wickham, J. (2007). Completion of  
724 the 2001 National Land Cover Database for the conterminous United States. *Photogrammetric*  
725 *Engineering and Remote Sensing*, 73(4), 5.

726 Huo, Z., Feng, S., Kang, S., Li, W., & Chen, S. (2008). Effect of climate changes and water-related  
727 human activities on annual stream flows of the Shiyang river basin in and north-west China.  
728 *Hydrological Processes*, 22(16), 3155–3167. <https://doi.org/10.1002/hyp.6900>

729 Jefferson, A. J., Bhaskar, A. S., Hopkins, K. G., Fanelli, R., Avellaneda, P. M., & McMillan, S. K.  
730 (2017). Stormwater management network effectiveness and implications for urban watershed  
731 function: a critical review. *Hydrological Processes*. <https://doi.org/10.1002/hyp.11347>

732 Jiang, C., Xiong, L., Wang, D., Liu, P., Guo, S., & Xu, C.-Y. (2015). Separating the impacts of climate  
733 change and human activities on runoff using the Budyko-type equations with time-varying  
734 parameters. *Journal of Hydrology*, 522, 326–338. <https://doi.org/10.1016/j.jhydrol.2014.12.060>

735 Jiang, S., Ren, L., Yong, B., Singh, V. P., Yang, X., & Yuan, F. (2011). Quantifying the effects of climate  
736 variability and human activities on runoff from the Laohahe basin in northern China using three  
737 different methods. *Hydrological Processes*, 25(16), 2492–2505. <https://doi.org/10.1002/hyp.8002>

738 Joo, E., Zeri, M., Hussain, M. Z., DeLucia, E. H., & Bernacchi, C. J. (2017). Enhanced evapotranspiration  
739 was observed during extreme drought from Miscanthus, opposite of other crops. *Global Change*  
740 *Biology Bioenergy*. <https://doi.org/10.1111/gcbb.12448>

741 Juckem, P. F., Hunt, R. J., Anderson, M. P., & Robertson, D. M. (2008). Effects of climate and land  
742 management change on streamflow in the Driftless Area of Wisconsin. *Journal of Hydrology*,  
743 355(1–4), 123–130. <https://doi.org/10.1016/j.jhydrol.2008.03.010>

744 Kucharik, C. J. (2003). Evaluation of a process-based agro-ecosystem model (Agro-IBIS) across the US  
745 Corn Belt: Simulations of the interannual variability in maize yield. *Earth Interactions*, 7, 14.

746 Kucharik, C. J., & Brye, K. R. (2003). Integrated BIOSphere Simulator (IBIS) yield and nitrate loss  
747 predictions for Wisconsin maize receiving varied amounts of nitrogen fertilizer. *Journal of*  
748 *Environmental Quality*, 32(1), 247–268.

749 Kucharik, C. J., Foley, J. A., Delire, C., Fisher, V. A., Coe, M. T., Lenters, J. D., ... Gower, S. T. (2000).  
750 Testing the performance of a dynamic global ecosystem model: Water balance, carbon balance,  
751 and vegetation structure. *Global Biogeochemical Cycles*, 14(3), 795–825.  
752 <https://doi.org/10.1029/1999GB001138>

753 Lathrop, R. C., & Carpenter, S. R. (2013). Water quality implications from three decades of phosphorus  
754 loads and trophic dynamics in the Yahara chain of lakes. *Inland Waters*, 4(1), 1–14.

755 Li, Z., Liu, W., Zhang, X., & Zheng, F. (2009). Impacts of land use change and climate variability on  
756 hydrology in an agricultural catchment on the Loess Plateau of China. *Journal of Hydrology*,  
757 377(1–2), 35–42. <https://doi.org/10.1016/j.jhydrol.2009.08.007>

758 Lim, K. J., Engel, B. A., Tang, Z., Choi, J., Kim, K.-S., Muthukrishnan, S., & Tripathy, D. (2005).  
759 Automated Web GIS Based Hydrograph Analysis Tool, WHAT. *JAWRA Journal of the American*  
760 *Water Resources Association*, 41(6), 1407–1416. [https://doi.org/10.1111/j.1752-](https://doi.org/10.1111/j.1752-1688.2005.tb03808.x)  
761 1688.2005.tb03808.x

762 Mango, L. M., Melesse, A. M., McClain, M. E., Gann, D., & Setegn, S. G. (2011). Land use and climate  
763 change impacts on the hydrology of the upper Mara River Basin, Kenya: results of a modeling  
764 study to support better resource management. *Hydrology and Earth System Sciences*, 15(7),  
765 2245–2258. <https://doi.org/10.5194/hess-15-2245-2011>

766 Marhaento, H., Booij, M. J., Rientjes, T. h. m., & Hoekstra, A. Y. (2017). Attribution of changes in the  
767 water balance of a tropical catchment to land use change using the SWAT model. *Hydrological*  
768 *Processes*, 31(11), 2029–2040. <https://doi.org/10.1002/hyp.11167>

769 Martin, K. L., Hwang, T., Vose, J. M., Coulston, J. W., Wear, D. N., Miles, B., & Band, L. E. (2017).  
770 Watershed impacts of climate and land use changes depend on magnitude and land use context.  
771 *Ecohydrology*, n/a-n/a. <https://doi.org/10.1002/eco.1870>

772 Menne, M. J., Durre, I., Vose, R. S., Gleason, B. E., & Houston, T. G. (2012). An Overview of the Global  
773 Historical Climatology Network-Daily Database. *Journal of Atmospheric and Oceanic*  
774 *Technology*, 29(7), 897–910. <https://doi.org/10.1175/JTECH-D-11-00103.1>

775 Milly, P. C. D., Betancourt, J., Falkenmark, M., Hirsch, R. M., Kundzewicz, Z. W., Lettenmaier, D. P., &  
776 Stouffer, R. J. (2008). Stationarity is dead: Whither water management? *Science*, 319(5863), 573–  
777 574. <https://doi.org/10.1126/science.1151915>

778 Moriasi, D. N., Arnold, J. G., Van Liew, M. W., Bingner, R. L., Harmel, R. D., & Veith, T. L. (2007).  
779 Model evaluation guidelines for systematic quantification of accuracy in watershed simulations.  
780 *Transactions of the ASABE*, 50(3), 885–900.

781 Motew, M., Chen, X., Booth, E. G., Carpenter, S. R., Pinkas, P., Zipper, S. C., ... Kucharik, C. J. (2017).  
782 The Influence of Legacy P on Lake Water Quality in a Midwestern Agricultural Watershed.  
783 *Ecosystems*, 1–15. <https://doi.org/10.1007/s10021-017-0125-0>

784 Newcomer, M. E., Gurdak, J. J., Sklar, L. S., & Nanus, L. (2014). Urban recharge beneath low impact  
785 development and effects of climate variability and change. *Water Resources Research*, 50(2),  
786 1716–1734. <https://doi.org/10.1002/2013WR014282>

787 Nosoetto, M. D., Jobbágy, E. G., Brizuela, A. B., & Jackson, R. B. (2012). The hydrologic consequences  
788 of land cover change in central Argentina. *Agriculture, Ecosystems & Environment*, 154, 2–11.  
789 <https://doi.org/10.1016/j.agee.2011.01.008>

790 Oliveira, P. T. S., Leite, M. B., Mattos, T., Nearing, M. A., Scott, R. L., de Oliveira Xavier, R., ...  
791 Wendland, E. (2017). Groundwater recharge decrease with increased vegetation density in the  
792 Brazilian cerrado. *Ecohydrology*, 10(1), e1759. <https://doi.org/10.1002/eco.1759>

793 Paturel, J. E., Mahé, G., Diello, P., Barbier, B., Dezetter, A., Dieulin, C., ... Maiga, A. (2017). Using land  
794 cover changes and demographic data to improve hydrological modeling in the Sahel.  
795 *Hydrological Processes*, 31(4), 811–824. <https://doi.org/10.1002/hyp.11057>

796 Peng, H., Tague, C., & Jia, Y. (2016). Evaluating the eco-hydrologic impacts of reforestation in the Loess  
797 Plateau, China, using an eco-hydrologic model. *Ecohydrology*, 9(3), 498–513.  
798 <https://doi.org/10.1002/eco.1652>

799 Peterson, H. M., Nieber, J. L., & Kanivetsky, R. (2011). Hydrologic regionalization to assess  
800 anthropogenic changes. *Journal of Hydrology*, 408(3), 212–225.  
801 <https://doi.org/10.1016/j.jhydrol.2011.07.042>

802 Pribulick, C. E., Foster, L. M., Bearup, L. A., Navarre-Sitchler, A. K., Williams, K. H., Carroll, R. W. H.,  
803 & Maxwell, R. M. (2016). Contrasting the hydrologic response due to land cover and climate  
804 change in a mountain headwaters system. *Ecohydrology*, 9(8), 1431–1438.  
805 <https://doi.org/10.1002/eco.1779>

806 Qiu, J., & Turner, M. G. (2013). Spatial interactions among ecosystem services in an urbanizing  
807 agricultural watershed. *Proceedings of the National Academy of Sciences*.  
808 <https://doi.org/10.1073/pnas.1310539110>

809 Qiu, J., & Turner, M. G. (2015). Importance of landscape heterogeneity in sustaining hydrologic  
810 ecosystem services in an agricultural watershed. *Ecosphere*, 6(11), 1–19.  
811 <https://doi.org/10.1890/ES15-00312.1>

812 Qiu, J., Wardropper, C. B., Rissman, A. R., & Turner, M. G. (2017). Spatial fit between water quality  
813 policies and hydrologic ecosystem services in an urbanizing agricultural landscape. *Landscape  
814 Ecology*, 32(1), 59–75. <https://doi.org/10.1007/s10980-016-0428-0>

815 R Core Team. (2017). R: A language and environment for statistical computing (Version 3.4.0). Vienna,  
816 Austria: R Foundation for Statistical Computing. Retrieved from <https://www.R-project.org/>

817 Robertson, W. M., Böhlke, J. K., & Sharp, J. M. (2017). Response of deep groundwater to land use  
818 change in desert basins of the Trans-Pecos region, Texas, USA: Effects on infiltration, recharge,  
819 and nitrogen fluxes. *Hydrological Processes*, 31(13), 2349–2364.  
820 <https://doi.org/10.1002/hyp.11178>

821 Rose, S., & Peters, N. E. (2001). Effects of urbanization on streamflow in the Atlanta area (Georgia,  
822 USA): a comparative hydrological approach. *Hydrological Processes*, 15(8), 1441–1457.  
823 <https://doi.org/10.1002/hyp.218>

824 Scanlon, B. R., Reedy, R. C., Stonestrom, D. A., Prudic, D. E., & Dennehy, K. F. (2005). Impact of land  
825 use and land cover change on groundwater recharge and quality in the southwestern US. *Global*  
826 *Change Biology*, *11*(10), 1577–1593. <https://doi.org/10.1111/j.1365-2486.2005.01026.x>

827 Schatz, J., & Kucharik, C. J. (2014). Seasonality of the urban heat island effect in Madison, Wisconsin.  
828 *Journal of Applied Meteorology and Climatology*, *53*(10), 2371–2386.  
829 <https://doi.org/10.1175/JAMC-D-14-0107.1>

830 Scheffer, M., Barrett, S., Carpenter, S. R., Folke, C., Green, A. J., Holmgren, M., ... Walker, B. (2015).  
831 Creating a safe operating space for iconic ecosystems. *Science*, *347*(6228), 1317–1319.  
832 <https://doi.org/10.1126/science.aaa3769>

833 Schott, L., Lagzdins, A., Daigh, A. L. M., Craft, K., Pederson, C., Brenneman, G., & Helmers, M. J.  
834 (2017). Drainage water management effects over five years on water tables, drainage, and yields  
835 in southeast Iowa. *Journal of Soil and Water Conservation*, *72*(3), 251–259.  
836 <https://doi.org/10.2489/jswc.72.3.251>

837 Schottler, S. P., Ulrich, J., Belmont, P., Moore, R., Lauer, J. W., Engstrom, D. R., & Almendinger, J. E.  
838 (2014). Twentieth century agricultural drainage creates more erosive rivers. *Hydrological*  
839 *Processes*, *28*(4), 1951–1961. <https://doi.org/10.1002/hyp.9738>

840 Schwartz, S. S., & Smith, B. (2014). Slowflow fingerprints of urban hydrology. *Journal of Hydrology*,  
841 *515*, 116–128. <https://doi.org/10.1016/j.jhydrol.2014.04.019>

842 Shi, P., Ma, X., Hou, Y., Li, Q., Zhang, Z., Qu, S., ... Fang, X. (2012). Effects of land-use and climate  
843 change on hydrological processes in the upstream of Huai River, China. *Water Resources*  
844 *Management*, *27*(5), 1263–1278. <https://doi.org/10.1007/s11269-012-0237-4>

845 Shuster, W. D., Darner, R. A., Schifman, L. A., & Herrmann, D. L. (2017). Factors Contributing to the  
846 Hydrologic Effectiveness of a Rain Garden Network (Cincinnati OH USA). *Infrastructures*, *2*(3),  
847 11. <https://doi.org/10.3390/infrastructures2030011>

848 Šimůnek, J., Šejna, M., Saito, H., Sakai, M., & van Genuchten, M. T. (2013). *The HYDRUS-1D Software*  
849 *Package for Simulating the One-Dimensional Movement of Water, Heat, and Multiple Solutes in*  
850 *Variably-Saturated Media, version 4.17*. Riverside, CA, USA: Department of Environmental  
851 Sciences, University of California Riverside.

852 Soylu, M. E., Kucharik, C. J., & Loheide, S. P. (2014). Influence of groundwater on plant water use and  
853 productivity: Development of an integrated ecosystem – Variably saturated soil water flow  
854 model. *Agricultural and Forest Meteorology*, *189–190*, 198–210.  
855 <https://doi.org/10.1016/j.agrformet.2014.01.019>

856 Steffen, W., Richardson, K., Rockström, J., Cornell, S. E., Fetzer, I., Bennett, E. M., ... Sörlin, S. (2015).  
857 Planetary boundaries: Guiding human development on a changing planet. *Science*, *347*(6223),  
858 1259855. <https://doi.org/10.1126/science.1259855>

859 Tang, Y., & Wang, D. (2017). Evaluating the role of watershed properties in long-term water balance  
860 through a Budyko equation based on two-stage partitioning of precipitation. *Water Resources*  
861 *Research*. <https://doi.org/10.1002/2016WR019920>

862 Tao, B., Tian, H., Ren, W., Yang, J., Yang, Q., He, R., ... Lohrenz, S. (2014). Increasing Mississippi  
863 River discharge throughout the 21st century influenced by changes in climate, land use, and  
864 atmospheric CO<sub>2</sub>. *Geophysical Research Letters*, *41*(14), 4978–4986.  
865 <https://doi.org/10.1002/2014GL060361>

866 The Inkscape Team. (2015). Inkscape (Version 0.91). Retrieved from <https://inkscape.org/en/>

- 867 Tomer, M. D., & Schilling, K. E. (2009). A simple approach to distinguish land-use and climate-change  
868 effects on watershed hydrology. *Journal of Hydrology*, 376(1–2), 24–33.  
869 <https://doi.org/10.1016/j.jhydrol.2009.07.029>
- 870 Twine, T. E., Kucharik, C. J., & Foley, J. A. (2004). Effects of land cover change on the energy and water  
871 balance of the Mississippi River basin. *Journal of Hydrometeorology*, 5(4), 640–655.  
872 [https://doi.org/10.1175/1525-7541\(2004\)005<0640:EOLCCO>2.0.CO;2](https://doi.org/10.1175/1525-7541(2004)005<0640:EOLCCO>2.0.CO;2)
- 873 Twine, T. E., Bryant, J. J., T. Richter, K., Bernacchi, C. J., McConnaughay, K. D., Morris, S. J., &  
874 Leakey, A. D. B. (2013). Impacts of elevated CO<sub>2</sub> concentration on the productivity and surface  
875 energy budget of the soybean and maize agroecosystem in the Midwest USA. *Global Change  
876 Biology*, 19(9), 2838–2852. <https://doi.org/10.1111/gcb.12270>
- 877 U.S. Geological Survey. (2017). National Water Information System. Retrieved May 9, 2017, from  
878 <https://waterdata.usgs.gov/nwis>
- 879 Usinowicz, J., Qiu, J., & Kamarainen, A. (2017). Flashiness and Flooding of Two Lakes in the Upper  
880 Midwest During a Century of Urbanization and Climate Change. *Ecosystems*, 20(3), 601–615.  
881 <https://doi.org/10.1007/s10021-016-0042-7>
- 882 VanLoocke, A., Bernacchi, C. J., & Twine, T. E. (2010). The impacts of *Miscanthus x giganteus*  
883 production on the Midwest US hydrologic cycle. *Global Change Biology Bioenergy*, 2(4), 180–  
884 191. <https://doi.org/10.1111/j.1757-1707.2010.01053.x>
- 885 Villarini, G., & Strong, A. (2014). Roles of climate and agricultural practices in discharge changes in an  
886 agricultural watershed in Iowa. *Agriculture Ecosystems & Environment*, 188, 204–211.  
887 <https://doi.org/10.1016/j.agee.2014.02.036>
- 888 Vörösmarty, C. J., Green, P., Salisbury, J., & Lammers, R. B. (2000). Global water resources:  
889 Vulnerability from climate change and population growth. *Science*, 289(5477), 284–288.  
890 <https://doi.org/10.1126/science.289.5477.284>
- 891 Wadzuk, B. M., Rea, M., Woodruff, G., Flynn, K., & Traver, R. G. (2010). Water-Quality Performance of  
892 a Constructed Stormwater Wetland for All Flow Conditions. *Journal of the American Water  
893 Resources Association*, 46(2), 385–394. <https://doi.org/10.1111/j.1752-1688.2009.00408.x>
- 894 Wagner, M., Wang, M., Miguez-Macho, G., Miller, J., VanLoocke, A., Bagley, J. E., ... Georgescu, M.  
895 (2017). A realistic meteorological assessment of perennial biofuel crop deployment: a Southern  
896 Great Plains perspective. *Global Change Biology Bioenergy*, 9(6), 1024–1041.  
897 <https://doi.org/10.1111/gcbb.12403>
- 898 Wang, D., & Hejazi, M. (2011). Quantifying the relative contribution of the climate and direct human  
899 impacts on mean annual streamflow in the contiguous United States. *Water Resources Research*,  
900 47(10), W00J12. <https://doi.org/10.1029/2010WR010283>
- 901 Wang, J., Sheng, Y., & Wada, Y. (2017). Little impact of the Three Gorges Dam on recent decadal lake  
902 decline across China's Yangtze Plain. *Water Resources Research*.  
903 <https://doi.org/10.1002/2016WR019817>
- 904 Wardropper, C. B., Chang, C., & Rissman, A. R. (2015). Fragmented water quality governance:  
905 Constraints to spatial targeting for nutrient reduction in a Midwestern USA watershed. *Landscape  
906 and Urban Planning*, 137, 64–75. <https://doi.org/10.1016/j.landurbplan.2014.12.011>
- 907 Wardropper, C. B., Gillon, S., Mase, A. S., McKinney, E. A., Carpenter, S. R., & Rissman, A. R. (2016).  
908 Local perspectives and global archetypes in scenario development. *Ecology and Society*, 21(2).  
909 <https://doi.org/10.5751/ES-08384-210212>

910 WICCI. (2011). *Wisconsin's Changing Climate: Impacts and Adaptation*. Madison, Wisconsin:  
911 Wisconsin Initiative on Climate Change Impacts, Nelson Institute for Environmental Studies,  
912 University of Wisconsin-Madison and the Wisconsin Department of Natural Resources.

913 Wickham, H. (2009). *ggplot2: Elegant Graphics for Data Analysis*. Springer-Verlag New York.  
914 Retrieved from <http://ggplot2.org>

915 Wisconsin Department of Natural Resources. (2016). Wisconsin land cover data - "Wiscland." Retrieved  
916 July 25, 2017, from <http://dnr.wi.gov/maps/gis/datalandcover.html>

917 Wu, C. S., Yang, S. L., & Lei, Y. (2012). Quantifying the anthropogenic and climatic impacts on water  
918 discharge and sediment load in the Pearl River (Zhujiang), China (1954-2009). *Journal of*  
919 *Hydrology*, 452, 190–204. <https://doi.org/10.1016/j.jhydrol.2012.05.064>

920 Wu, F., Zhan, J., Su, H., Yan, H., & Ma, E. (2015). Scenario-based impact assessment of land use/cover  
921 and climate changes on watershed hydrology in Heihe River Basin of Northwest China. *Advances*  
922 *in Meteorology*, 410198. <https://doi.org/10.1155/2015/410198>

923 Xu, X., Scanlon, B. R., Schilling, K., & Sun, A. (2013). Relative importance of climate and land surface  
924 changes on hydrologic changes in the US Midwest since the 1930s: Implications for biofuel  
925 production. *Journal of Hydrology*, 497, 110–120. <https://doi.org/10.1016/j.jhydrol.2013.05.041>

926 Yang, L., Feng, Q., Yin, Z., Wen, X., Si, J., Li, C., & Deo, R. C. (2017). Identifying separate impacts of  
927 climate and land use/cover change on hydrological processes in upper stream of Heihe River,  
928 Northwest China. *Hydrological Processes*, 31(5), 1100–1112. <https://doi.org/10.1002/hyp.11098>

929 Ye, B. S., Yang, D. Q., & Kane, D. L. (2003). Changes in Lena River streamflow hydrology: Human  
930 impacts versus natural variations. *Water Resources Research*, 39(7), 1200.  
931 <https://doi.org/10.1029/2003WR001991>

932 Zhang, Q., Liu, J., Singh, V. P., Gu, X., & Chen, X. (2016). Evaluation of impacts of climate change and  
933 human activities on streamflow in the Poyang Lake basin, China. *Hydrological Processes*,  
934 30(14), 2562–2576. <https://doi.org/10.1002/hyp.10814>

935 Zimmerman, B. G., Vimont, D. J., & Block, P. J. (2016). Utilizing the state of ENSO as a means for  
936 season-ahead predictor selection. *Water Resources Research*, 52(5), 3761–3774.  
937 <https://doi.org/10.1002/2015WR017644>

938 Zipper, S. C., Soyulu, M. E., Kucharik, C. J., & Loheide II, S. P. (2017a). Quantifying indirect  
939 groundwater-mediated effects of urbanization on agroecosystem productivity using MODFLOW-  
940 AgroIBIS (MAGI), a complete critical zone model. *Ecological Modelling*, 359, 201–219.  
941 <https://doi.org/10.1016/j.ecolmodel.2017.06.002>

942 Zipper, S. C., & Loheide, S. P. (2014). Using evapotranspiration to assess drought sensitivity on a  
943 subfield scale with HRMET, a high resolution surface energy balance model. *Agricultural and*  
944 *Forest Meteorology*, 197, 91–102. <https://doi.org/10.1016/j.agrformet.2014.06.009>

945 Zipper, S. C., Soyulu, M. E., Booth, E. G., & Loheide, S. P. (2015). Untangling the effects of shallow  
946 groundwater and soil texture as drivers of subfield-scale yield variability. *Water Resources*  
947 *Research*, 51(8), 6338–6358. <https://doi.org/10.1002/2015WR017522>

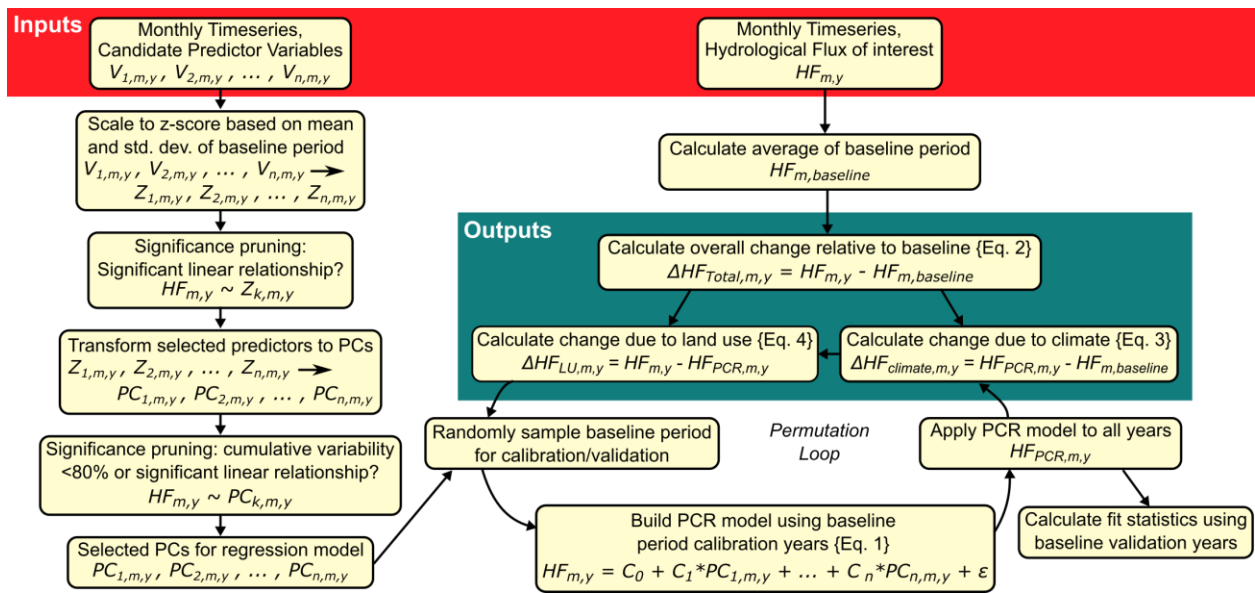
948 Zipper, S. C., Schatz, J., Singh, A., Kucharik, C. J., Townsend, P. A., & Loheide, S. P. (2016). Urban heat  
949 island impacts on plant phenology: intra-urban variability and response to land cover.  
950 *Environmental Research Letters*, 11(5), 054023. <https://doi.org/10.1088/1748-9326/11/5/054023>

951 Zipper, S. C., Schatz, J., Kucharik, C. J., & Loheide, S. P. (2017b). Urban heat island-induced increases  
952 in evapotranspirative demand. *Geophysical Research Letters*, 44(2), 2016GL072190.  
953 <https://doi.org/10.1002/2016GL072190>



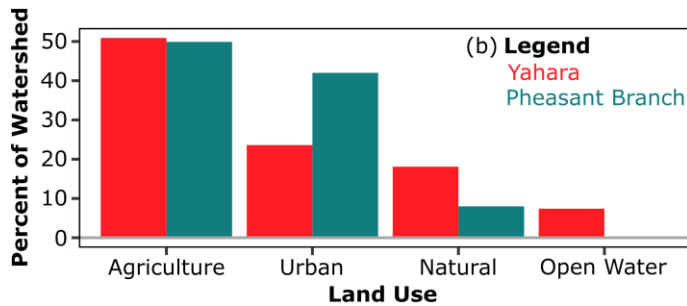
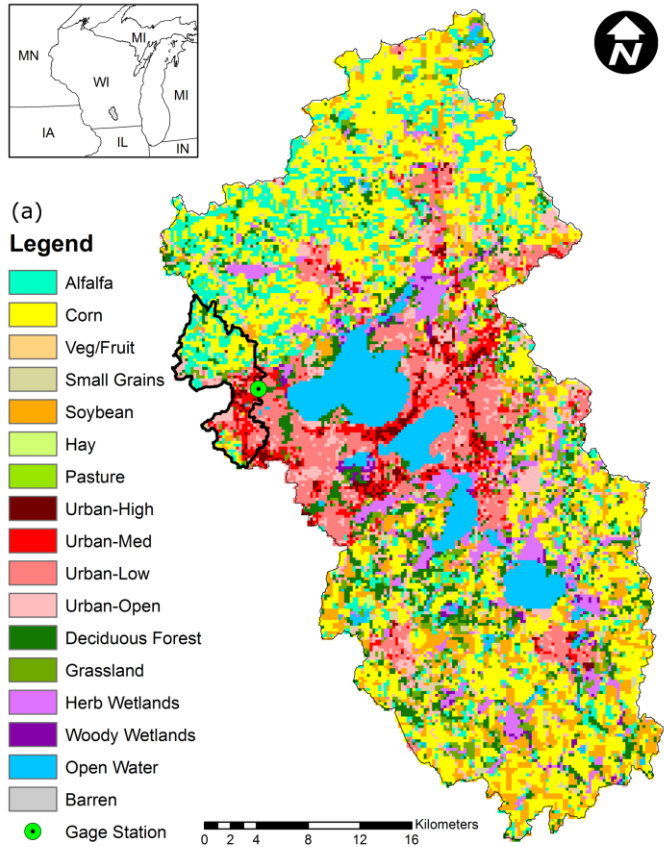
954

955 Figures & Tables



956  
957  
958  
959

**Figure 1.** Flowchart illustrating method for separating land use and climate effects, demonstrating the monthly resolution used in the current study.



960  
961  
962  
963  
964  
965  
966  
967

**Figure 2.** (a) Map of Yahara Watershed showing land use in 2014 at model resolution (220 m grid cells). The green dot shows the Pheasant Branch gauging station, and thick black line outlines the contributing area. (b) Relative proportion of different land uses in the Yahara River Watershed and Pheasant Branch Subwatershed. The Agriculture class includes all crops and pasture (top 7 legend entries in panel a). The Urban class includes all urban density levels as well as barren land. Natural includes forest, grassland, and wetlands.

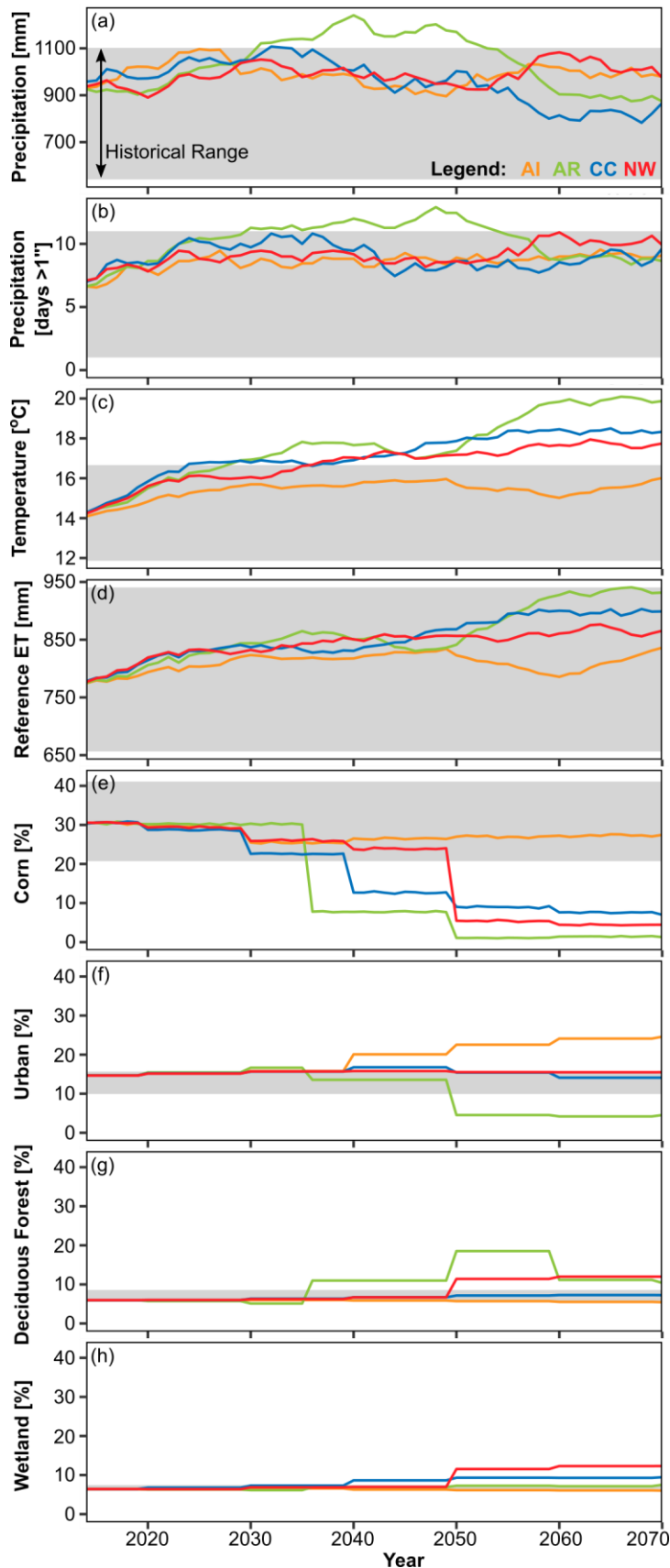
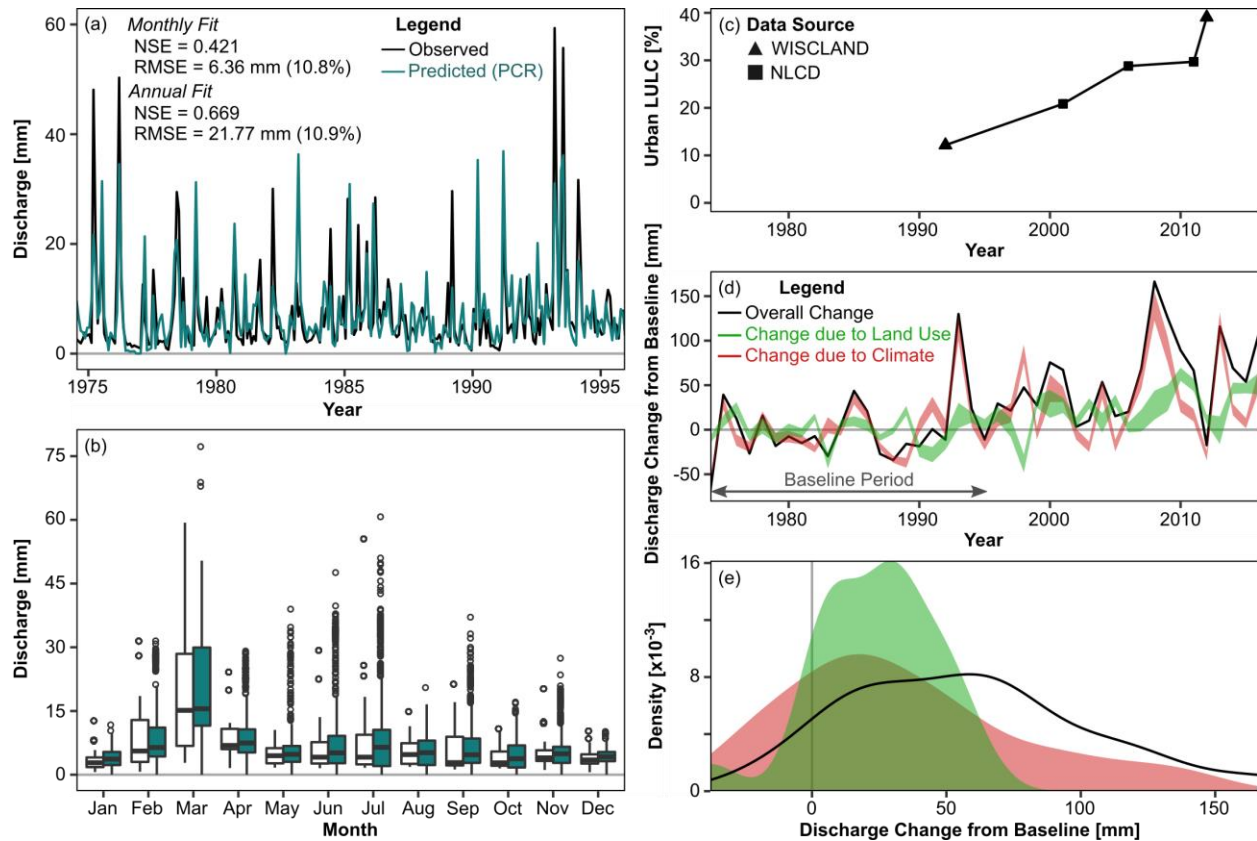
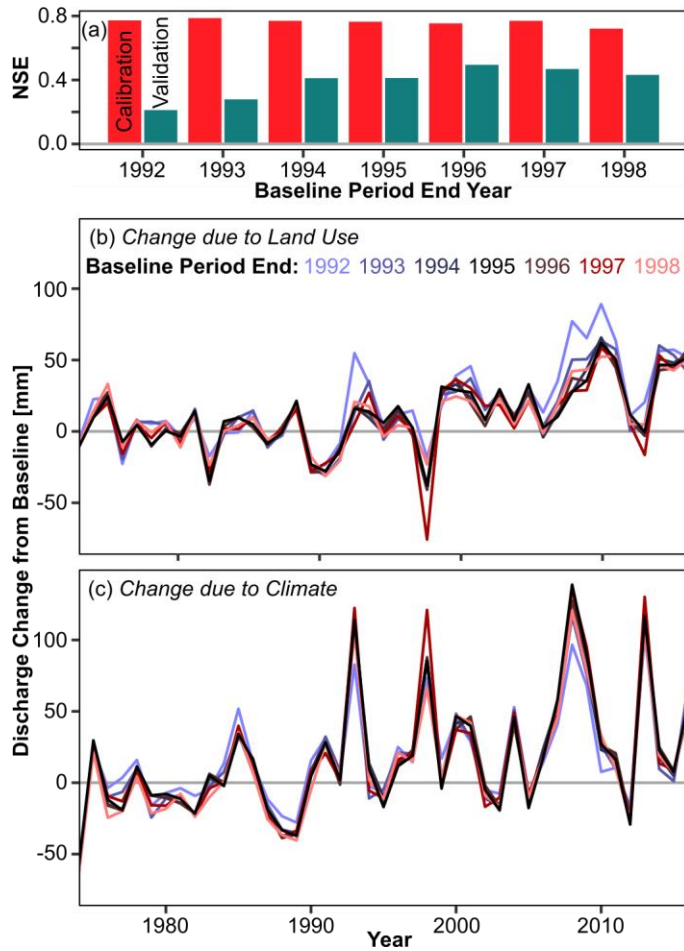


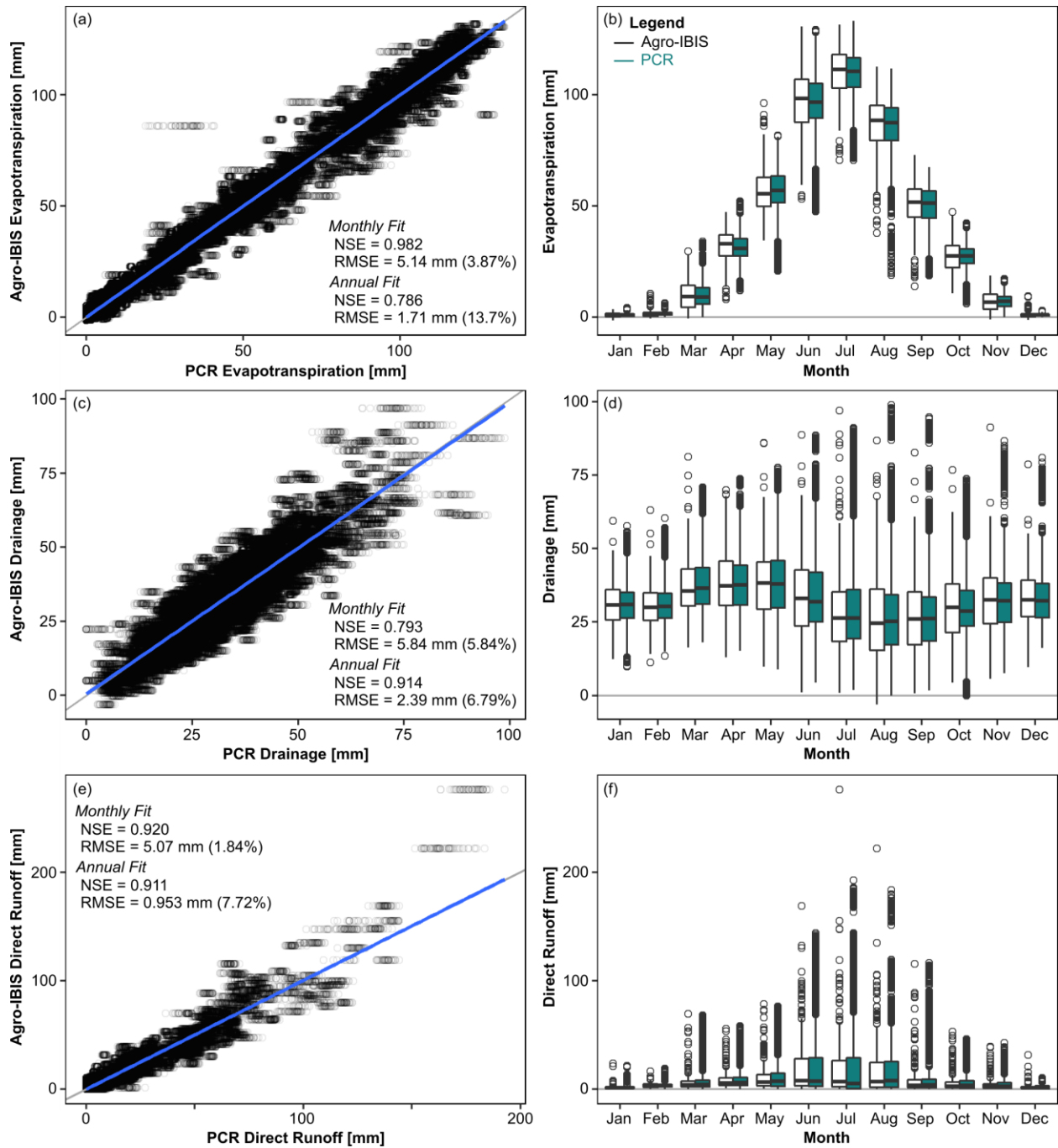
**Figure 3.** Annual watershed-average meteorological (a-d) and land use (e-h) model input for the four scenarios. In each plot, the gray shading represents the historical (1986-2013) range. Meteorological variables (a-d) are smoothed with an 11-year moving average. Plot show (a) annual cumulative precipitation; (b) annual days with >1'' (25.4 mm) precipitation; (c) mean maximum daily temperature; (d) mean Penman-Monteith reference evapotranspiration; (e) percent of domain with corn land cover; (f) percent of domain with urban (low, medium, and high density) land cover; (g) percent of domain with deciduous forest land cover; (h) percent of domain with wetland land cover.



988  
 989 **Figure 4.** Results from analysis of Pheasant Branch historical discharge data. (a) Comparison between  
 990 observed and predicted (mean of random validation samples for all PCR permutations) for baseline  
 991 period; (b) boxplots showing monthly distributions of discharge for observed (all years) and predicted (all  
 992 years and all permutations); (c) percent of Pheasant Branch Watershed with urban land use (combined  
 993 high, medium, and low density) from WISCLAND (Wisconsin Department of Natural Resources, 2016)  
 994 and NLCD datasets (Fry et al., 2011; Homer et al., 2007, 2015); (d) change relative to baseline period,  
 995 with solid line showing overall change and ribbons spanning  $\pm 1$  standard deviation of the mean across  
 996 all permutations; (e) density plot of mean annual changes in discharge due to land use, climate, and  
 997 overall. Legend in (a) also applies to (b) and legend in (d) also applies to (e).  
 998

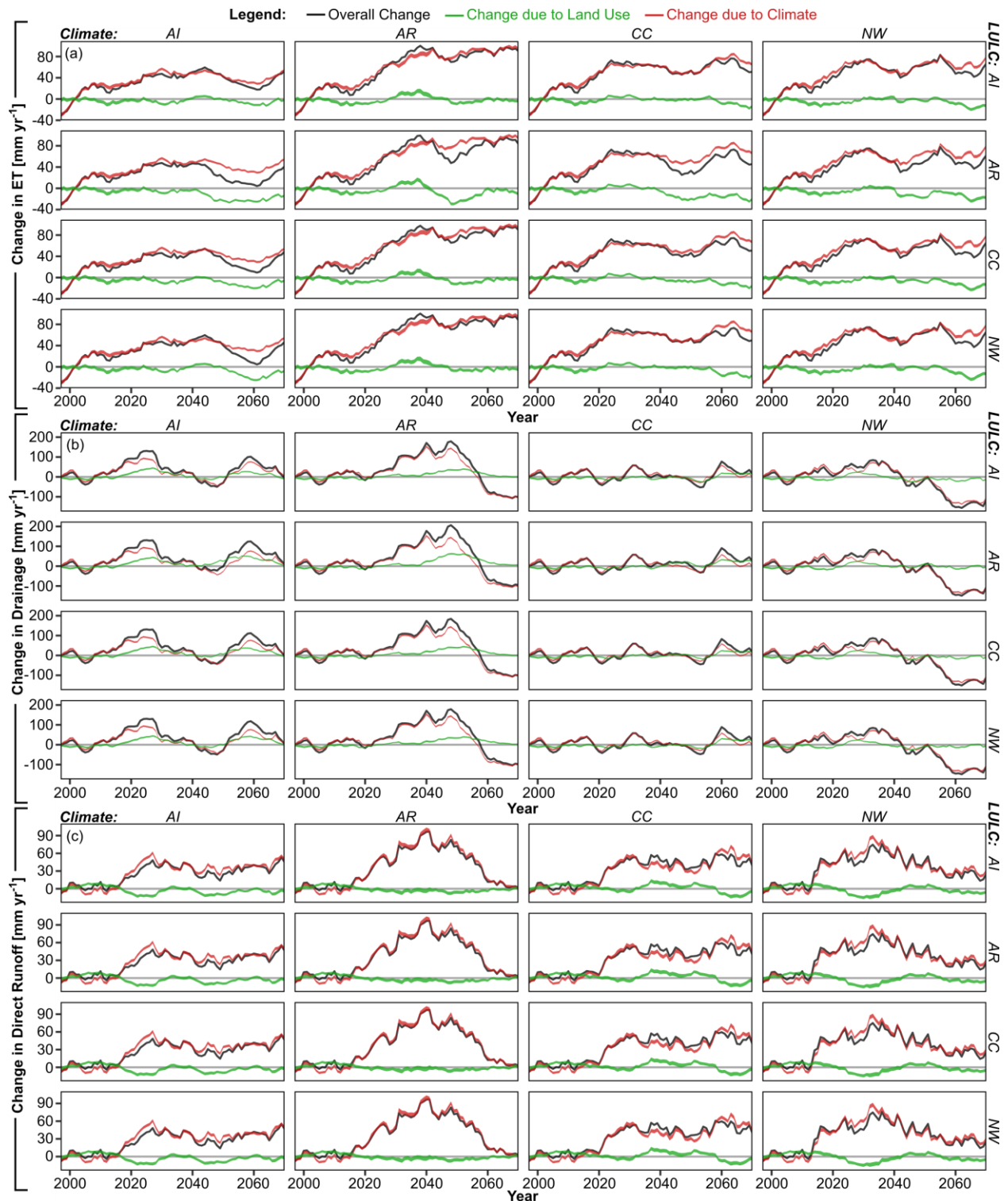


999  
 1000 **Figure 5.** Sensitivity of results for Pheasant Branch watershed to selection of baseline period. (a) Nash-  
 1001 Sutcliffe Efficiency for the calibration and validation samples as a function of the end of the baseline  
 1002 period. Changes in discharge due to (b) land use and (c) climate, color-coded by the end of the baseline  
 1003 period. All baseline periods begin in 1974. For results in Figure 4 and discussed in text, baseline period  
 1004 ends in 1995 (black line).

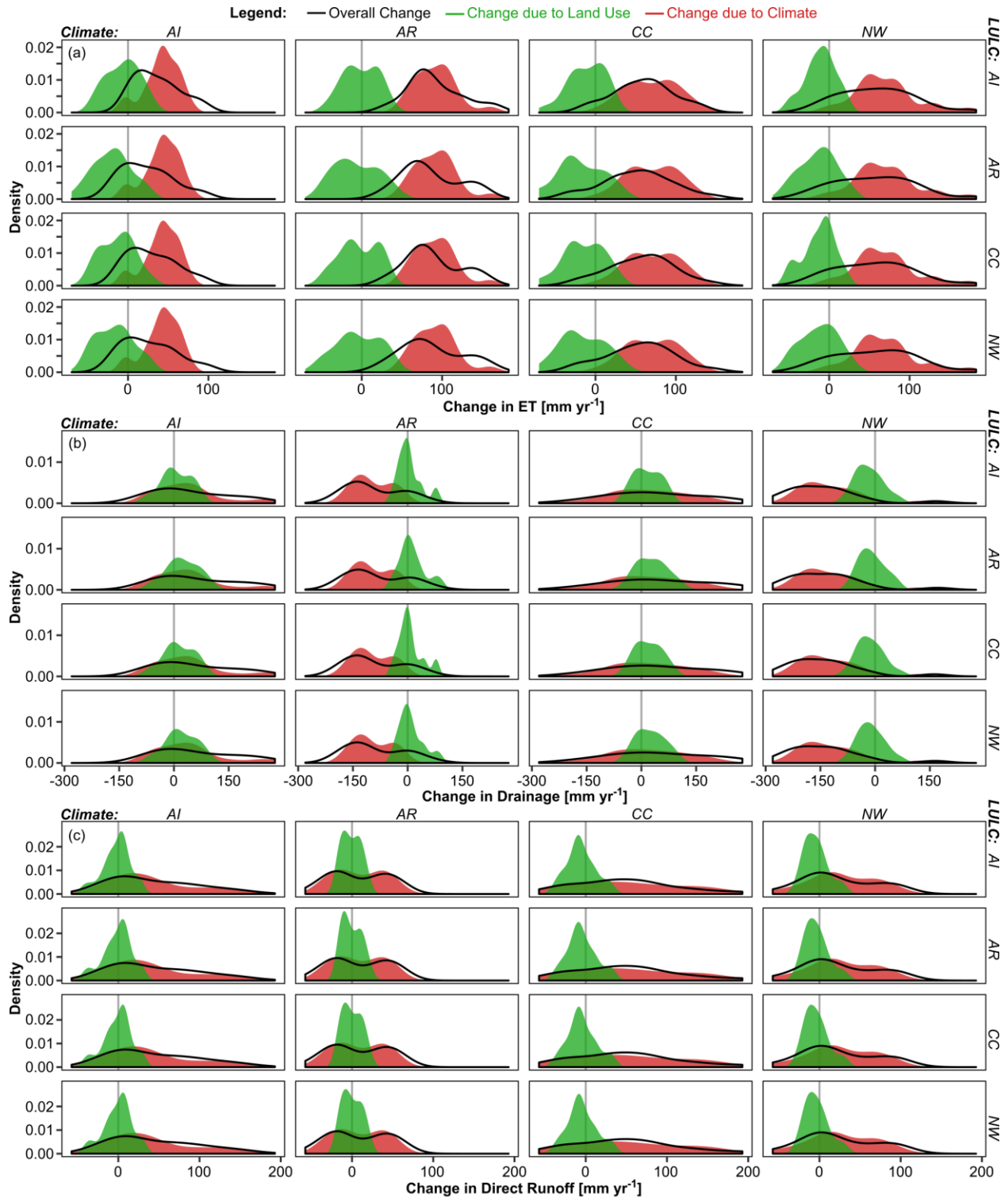


1005  
 1006  
 1007  
 1008

**Figure 6.** Validation of PCR relationships for (a,b) evapotranspiration, (c,d) drainage, and (e,f) direct runoff.



1009  
 1010 **Figure 7.** Changes from 1986-2013 baseline period for watershed-average annual (a) evapotranspiration,  
 1011 (b) drainage, and (c) direct runoff. In each set of 16 plots, the labels along the top show the climate  
 1012 scenario and the labels along the right side show the land use scenario. Ribbons for climate (red) and land  
 1013 use (green) show +/- 1 standard deviation of the mean across all permutations; lines and ribbons are  
 1014 smoothed using 11-year moving average.



1015  
 1016 **Figure 8.** Density plots showing distribution of overall (black line), climate-induced (shaded red), and  
 1017 land use-induced (shaded green) changes to annual watershed-average (a) evapotranspiration, (b)  
 1018 drainage, and (c) direct runoff. Distributions are for the final 20 years of the simulation (2051-2070),  
 1019 relative to the baseline period (1986-2013). In each set of 16 plots, the labels along the top show the  
 1020 climate scenario and the labels along the right side show the land use scenario.

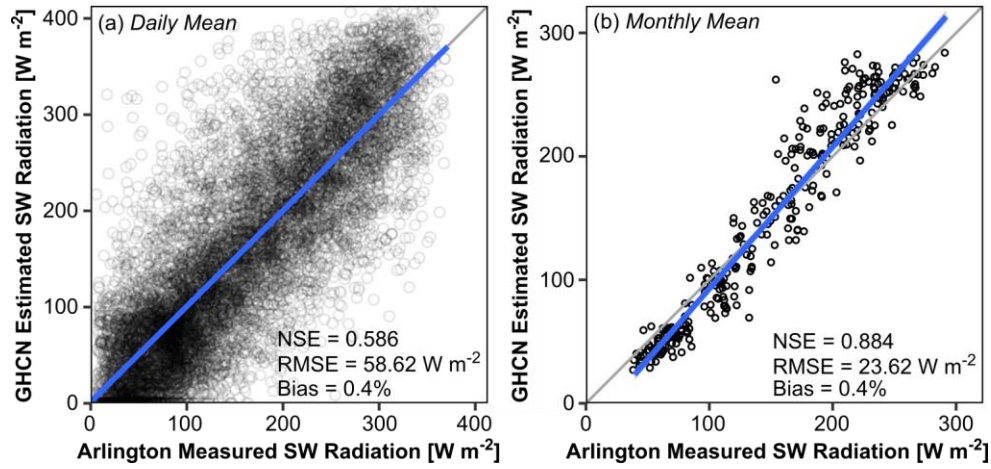


1021 **Supporting Information for Zipper et al., “Continuous separation of land use**  
 1022 **and climate effects on the water balance using principal components**  
 1023 **regression”**

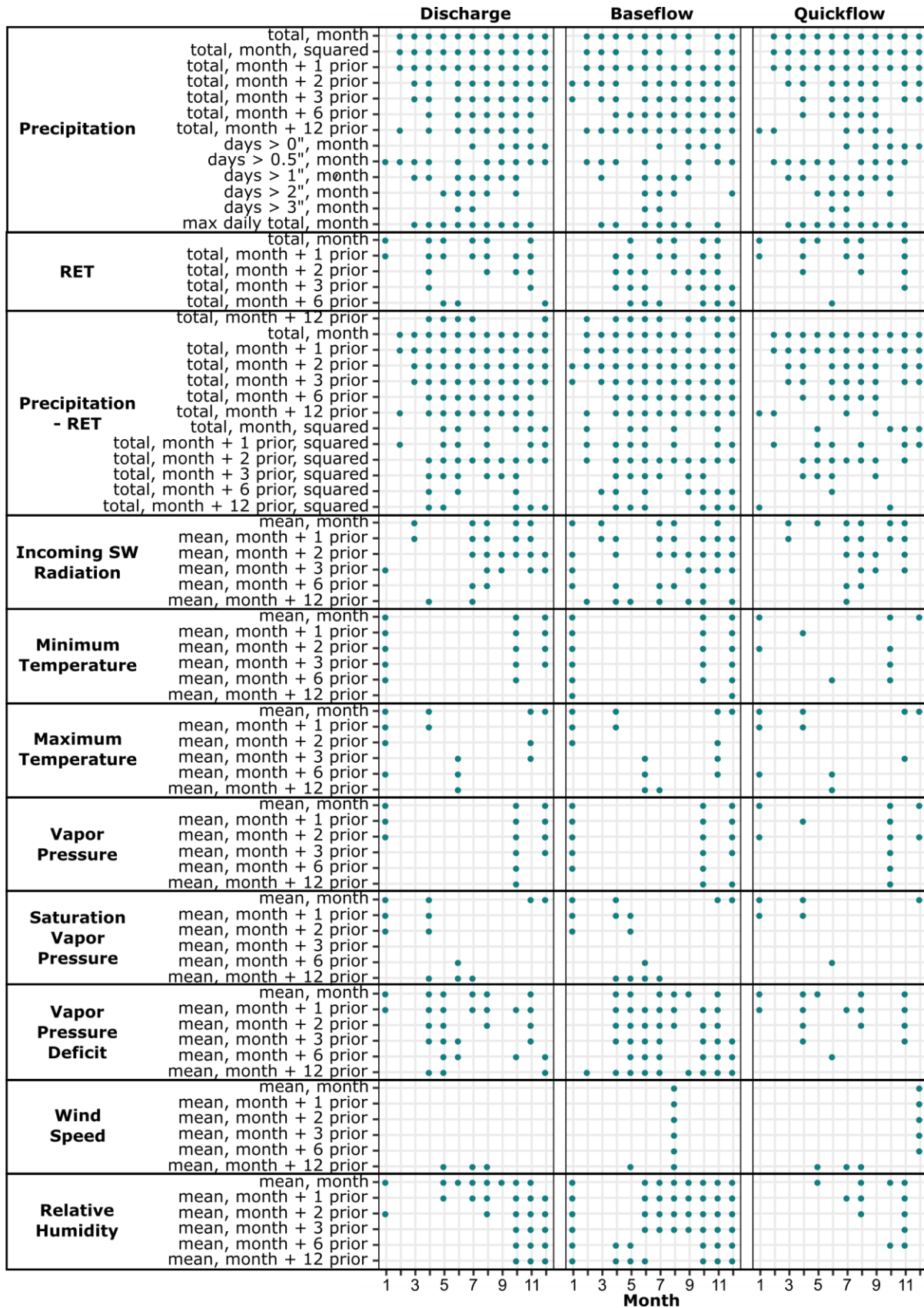
1024  
 1025 **Table S1.** PCR fit metrics for evapotranspiration (ET), drainage (DR), and direct runoff (RO) for future  
 1026 scenario analysis. Data shown are for all validation samples from all permutations during baseline period.  
 1027 NSE=Nash-Sutcliffe Efficiency, RMSE=Root Mean Squared Error, NRMSE=Normalized Root Mean  
 1028 Squared Error.

Month	NSE			RMSE			NRMSE		
	ET	DR	RO	ET	DR	RO	ET	DR	RO
1	0.529	0.724	0.793	0.666	4.129	1.010	13.4%	8.8%	4.3%
2	0.128	0.721	0.666	1.653	3.996	1.428	14.9%	7.7%	8.7%
3	0.758	0.827	0.866	3.045	4.224	3.426	10.0%	6.5%	4.9%
4	0.650	0.865	0.934	4.461	4.115	2.299	11.3%	7.2%	4.2%
5	0.640	0.839	0.924	6.628	5.102	3.668	10.7%	6.7%	4.7%
6	0.720	0.802	0.943	7.741	6.497	6.685	10.0%	7.4%	4.0%
7	0.676	0.782	0.889	6.521	7.517	10.700	10.7%	7.8%	3.9%
8	0.641	0.780	0.913	8.138	7.353	8.099	10.9%	8.2%	3.7%
9	0.676	0.726	0.908	6.070	7.108	4.952	10.3%	8.7%	4.3%
10	0.493	0.699	0.919	4.938	6.740	2.592	13.5%	9.3%	4.9%
11	0.565	0.721	0.649	2.943	6.215	3.699	14.8%	7.3%	9.4%
12	0.057	0.714	0.377	1.394	5.365	2.351	13.0%	7.8%	7.5%
<b>Overall</b>	<b>0.983</b>	<b>0.793</b>	<b>0.920</b>	<b>5.138</b>	<b>5.845</b>	<b>5.073</b>	<b>3.9%</b>	<b>5.8%</b>	<b>1.8%</b>

1030  
 1031

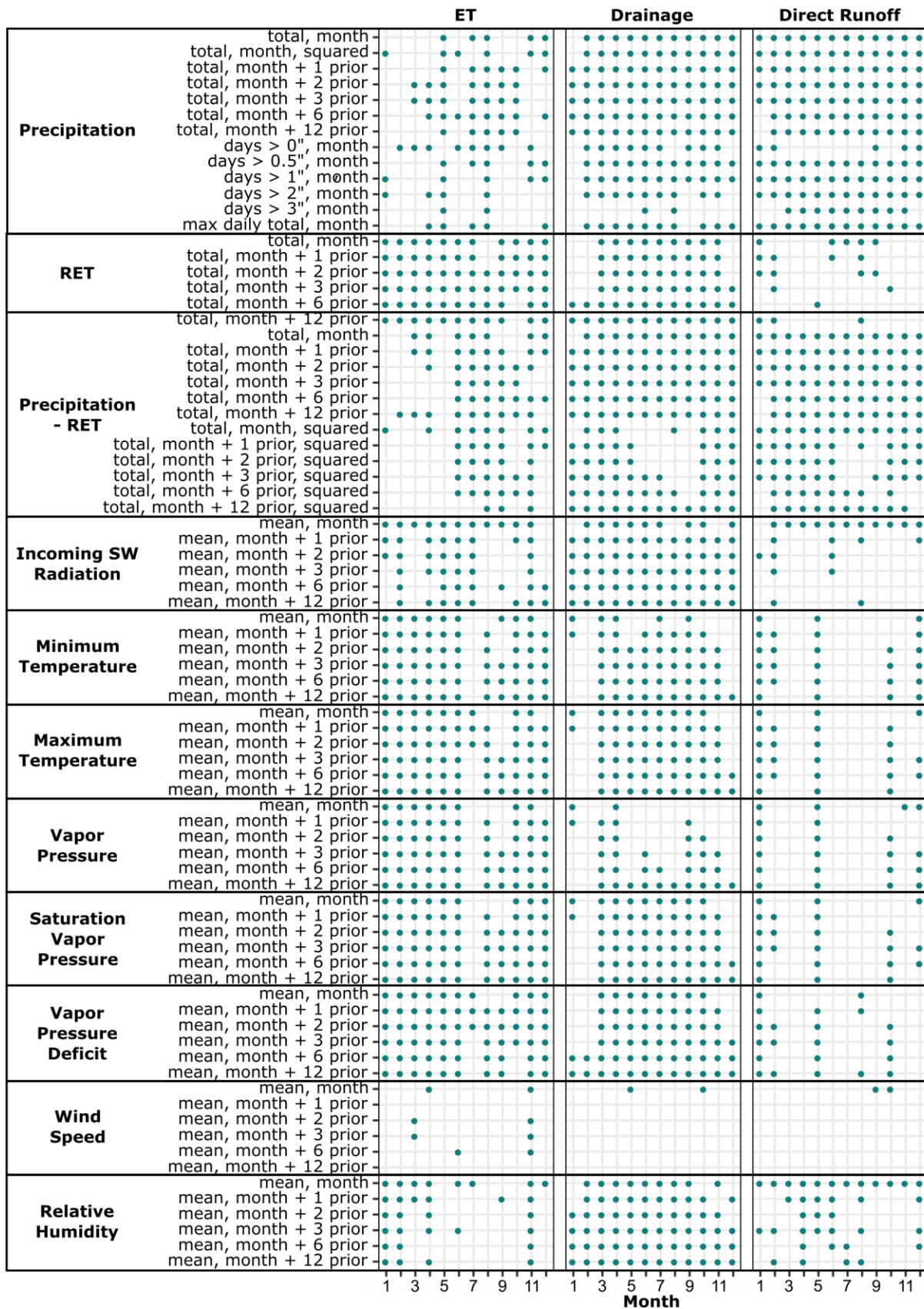


1032  
 1033 **Figure S1.** Comparison between (a) daily mean and (b) monthly mean incoming shortwave radiation.  
 1034 Arlington data are from agricultural weather station at Arlington Agricultural Research Station. GHCN  
 1035 data are estimated using daily maximum and minimum temperatures from a calibrated Bristow-Campbell  
 1036 equation (Bristow & Campbell, 1984).



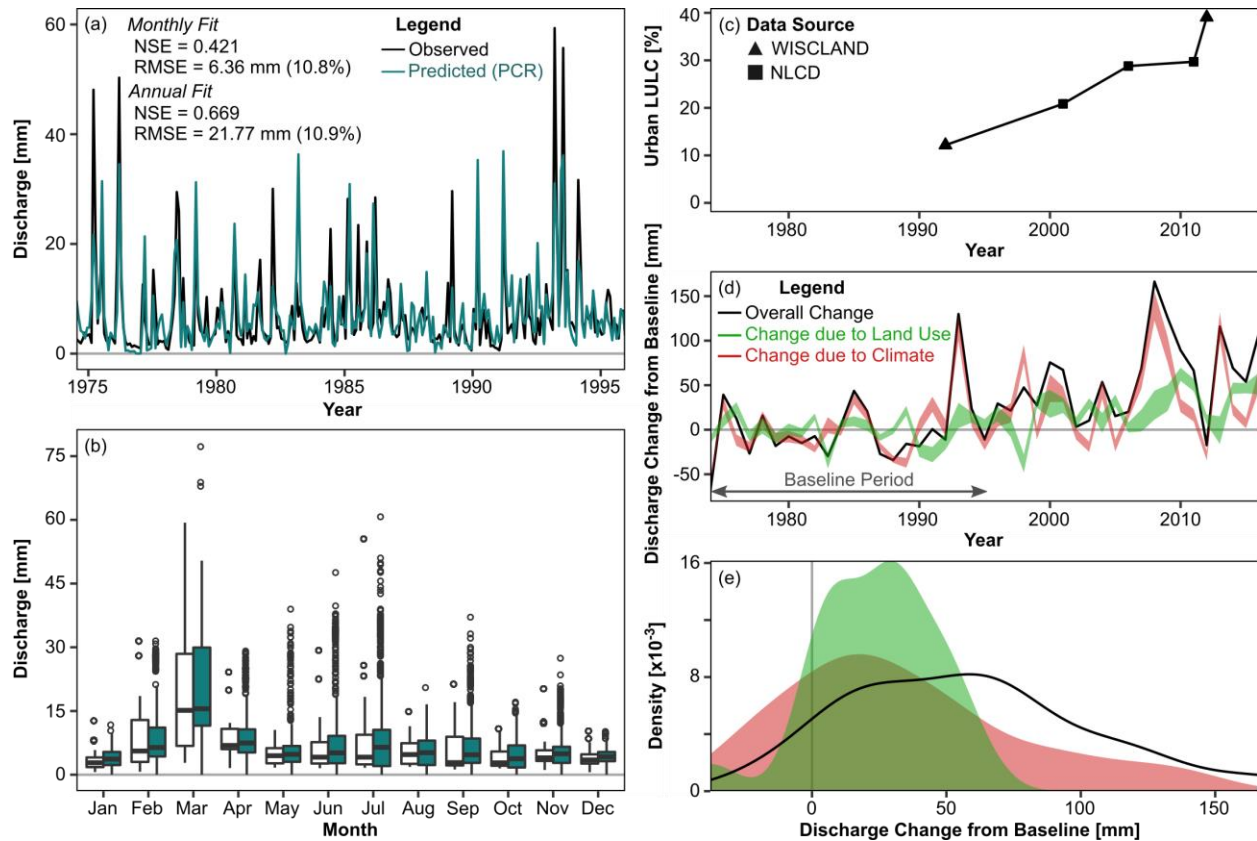
1037  
1038

**Figure S2.** Variables retained for Pheasant Branch analysis by month and hydrological flux.



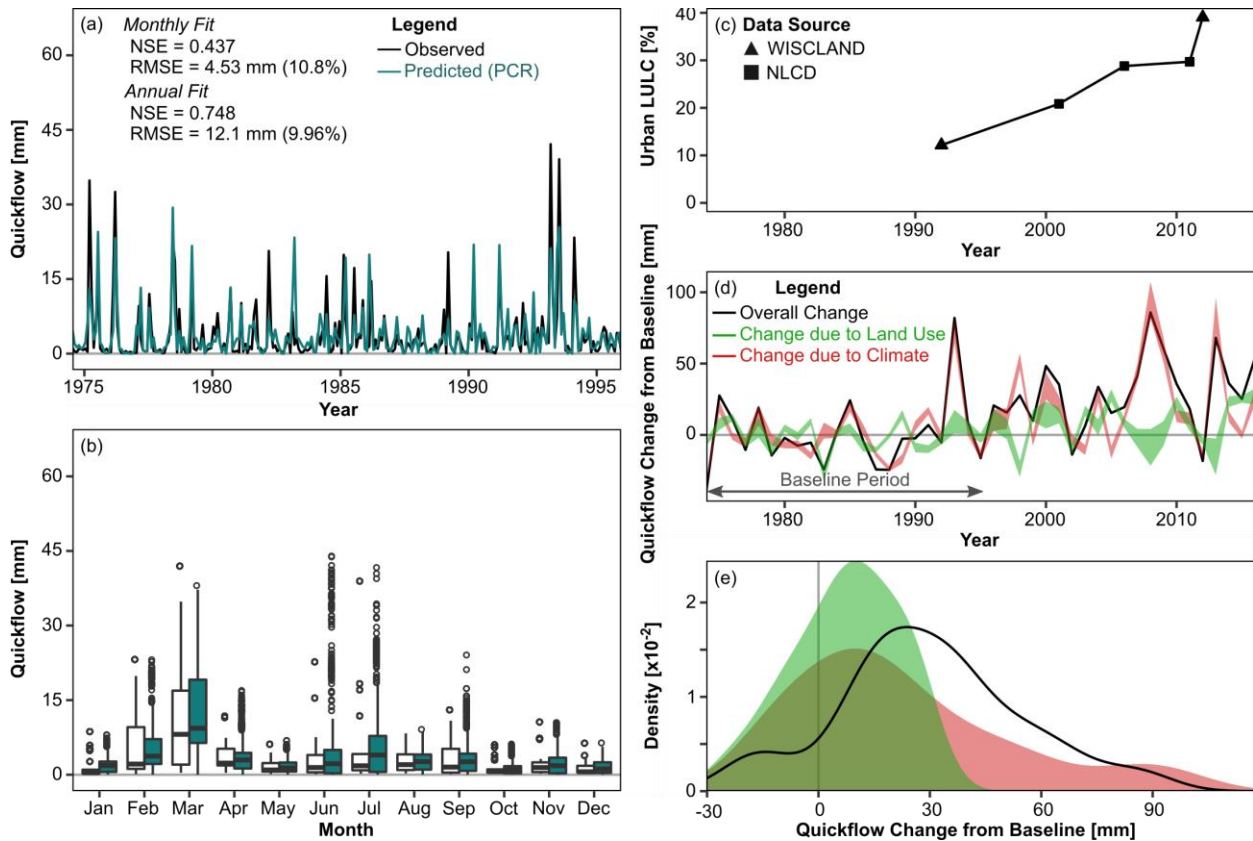
1039  
1040

Figure S3. Variables retained for Yahara Watershed analysis by month and hydrological flux.

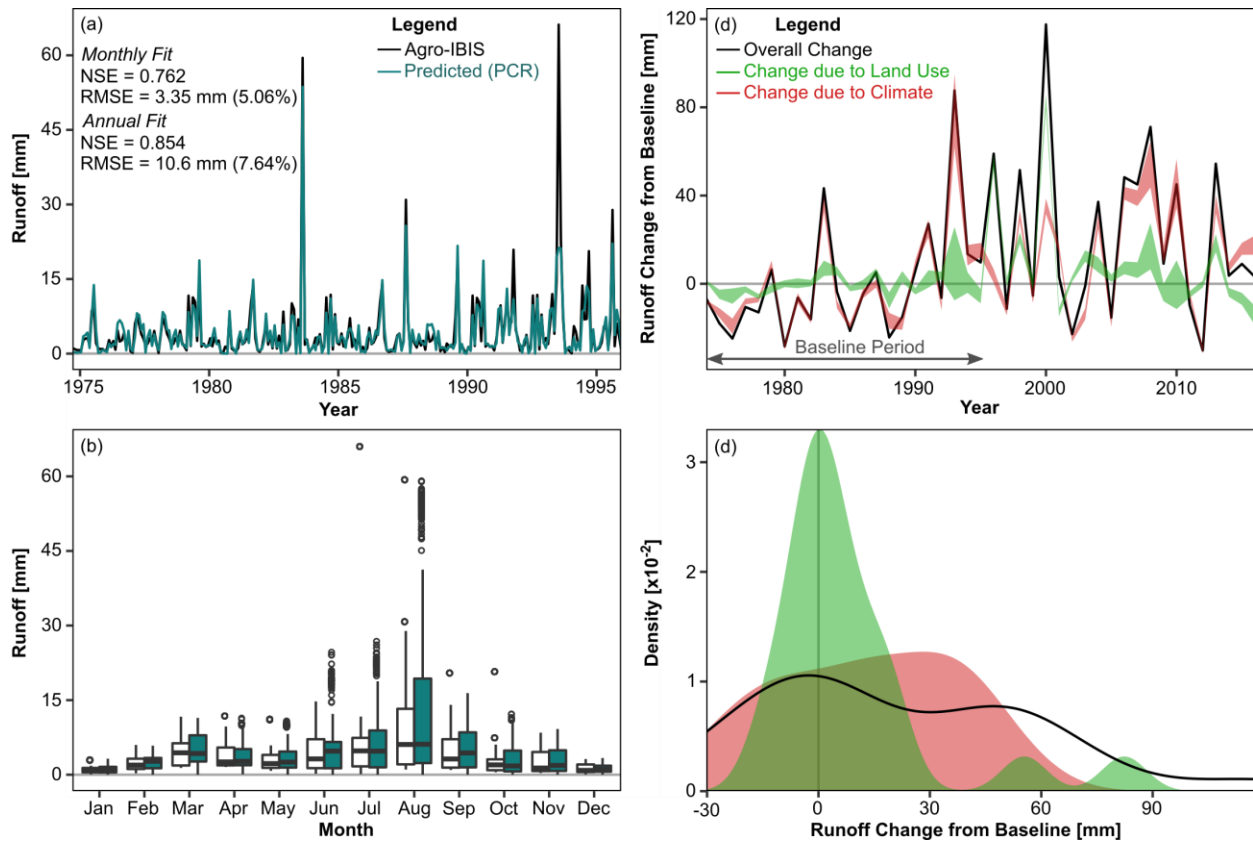


1041 **Figure S4 (as Figure 4, but for baseflow).** Results from analysis of Pheasant Branch historical baseflow  
 1042 data. (a) Comparison between observed and predicted (mean of random validation samples for all PCR  
 1043 permutations) for baseline period; (b) boxplots showing monthly distributions of baseflow for observed  
 1044 (all years) and predicted (all years and all permutations); (c) percent of Pheasant Branch Watershed with  
 1045 urban land use (combined high, medium, and low density) from WISCLAND (Wisconsin Department of  
 1046 Natural Resources, 2016) and NLCD datasets (Fry et al., 2011; Homer et al., 2007, 2015); (d) change  
 1047 relative to baseline period, with solid line showing overall change and ribbons spanning +/- 1 standard  
 1048 deviation of the mean across all permutations; (e) density plot of mean annual changes in baseflow due to  
 1049 land use, climate, and overall. Legend in (a) also applies to (b) and legend in (d) also applies to (e).  
 1050

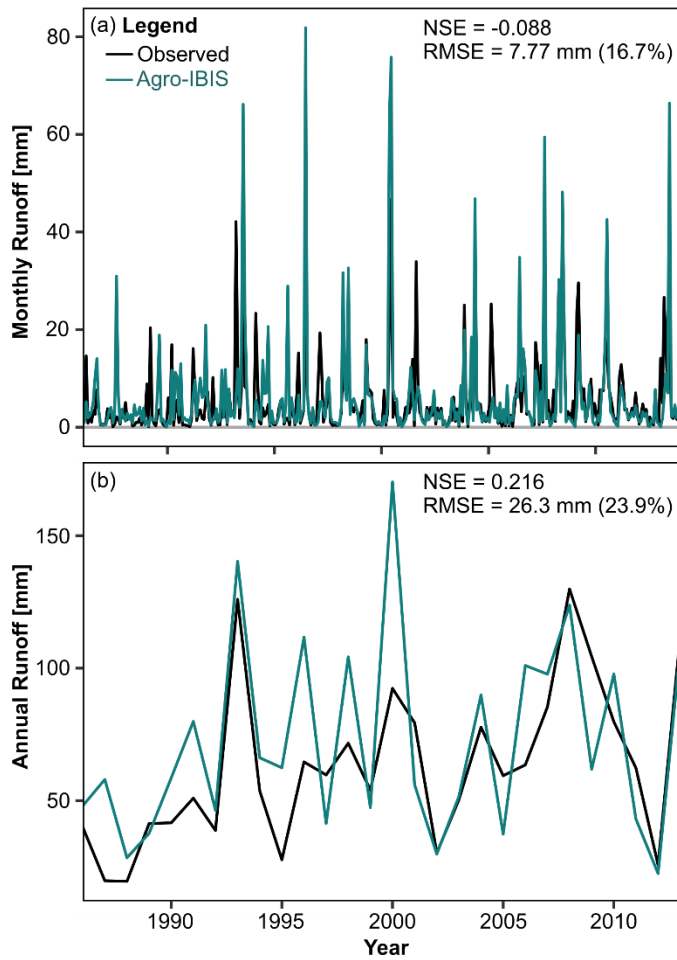
1051



1052  
 1053 **Figure S5 (as Figure 4, but for quickflow).** Results from analysis of Pheasant Branch historical  
 1054 quickflow data. (a) Comparison between observed and predicted (mean of random validation samples for  
 1055 all PCR permutations) for baseline period; (b) boxplots showing monthly distributions of quickflow for  
 1056 observed (all years) and predicted (all years and all permutations); (c) percent of Pheasant Branch  
 1057 Watershed with urban land use (combined high, medium, and low density) from WISCLAND (Wisconsin  
 1058 Department of Natural Resources, 2016) and NLCD datasets (Fry et al., 2011; Homer et al., 2007, 2015);  
 1059 (d) change relative to baseline period, with solid line showing overall change and ribbons spanning  $\pm 1$   
 1060 standard deviation of the mean across all permutations; (e) density plot of mean annual changes in  
 1061 quickflow due to land use, climate, and overall. Legend in (a) also applies to (b) and legend in (d) also  
 1062 applies to (e).



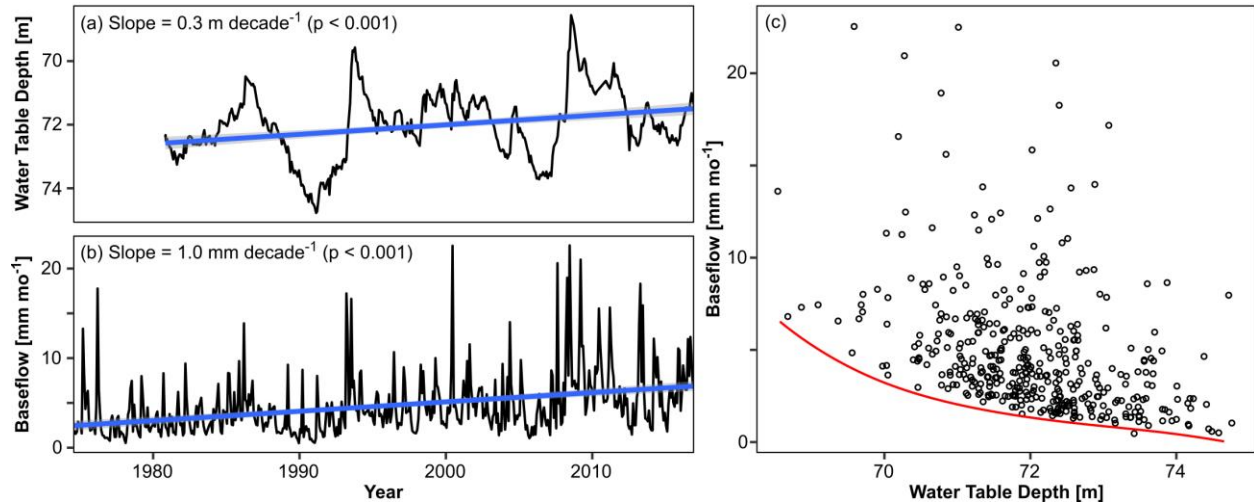
1063  
 1064 **Figure S6 (as Figure S5, but for Agro-IBIS simulated direct runoff in PBS).** Results from analysis of  
 1065 Agro-IBIS-simulated Pheasant Branch direct runoff from 1974-2016. (a) Comparison between observed  
 1066 and predicted (mean of random validation samples for all PCR permutations) for baseline period; (b)  
 1067 boxplots showing monthly distributions of direct runoff for observed (all years) and predicted (all years  
 1068 and all permutations); (c) change relative to baseline period, with solid line showing overall change and  
 1069 ribbons spanning +/- 1 standard deviation of the mean across all permutations; (d) density plot of mean  
 1070 annual changes in direct runoff due to land use, climate, and overall. Legend in (a) also applies to (b) and  
 1071 legend in (c) also applies to (d).



1072  
 1073  
 1074  
 1075  
 1076  
 1077

**Figure S7.** Comparison of simulated and observed direct runoff at (a) monthly and (b) annual timescales for the Pheasant Branch subwatershed. Observed runoff is quickflow estimated from overall discharge at the Pheasant Branch gauging station using baseflow separation. Agro-IBIS runoff is the average of direct runoff at all grid cells within the contributing area of the Pheasant Branch gauging station.





1078  
 1079  
 1080  
 1081  
 1082  
 1083  
 1084

**Figure S8.** (a) Water table depth at a well just north of the Pheasant Branch subwatershed in an area that has seen minimal urbanization (USGS 430638089353101); (b) estimated monthly baseflow in the Pheasant Branch watershed; and (c) baseflow as a function of water table depth. Blue lines in (a-b) show linear best-fit with 95% confidence interval. Red line in (c) shows the lower bound of baseflow increasing nonlinearly as a function of water table depth.